

Variations in Cortical Material Properties Throughout the Human Dentate Mandible

C.L. Schwartz-Dabney¹ and P.C. Dechow^{2*}

¹*Division of Oral and Maxillofacial Surgery, University of Texas Southwestern Medical Center, Dallas, Texas 75390-9109*

²*Department of Biomedical Sciences, Baylor College of Dentistry, Texas A&M University System Health Science Center, Dallas, Texas 75246*

KEY WORDS ultrasound; bone; biomechanics; development; function

ABSTRACT Material properties and their variations in individual bone organs are important for understanding bone adaptation and quality at a tissue level, and are essential for accurate mechanical models. Yet material property variations have received little systematic study. Like all other material property studies in individual bone organs, studies of the human mandible are limited by a low number of both specimens and sampled regions. The aims of this study were to determine: 1) regional variability in mandibular material properties, 2) the effect of this variability on the modeling of mandibular function, and 3) the relationship of this variability to mandibular structure and function. We removed 31 samples on both facial and lingual cortices of 10 fresh adult dentate mandibles, measured cortical thickness and density, determined the directions of maximum stiffness with a pulse transmission ultrasonic technique, and calculated elastic properties from measured ultrasonic velocities. Results showed that each of these elastic properties in the dentate human mandible demonstrates unique regional variation. The direction of maximum stiffness was near parallel to the occlusal plane within the corpus. On the facial ramus, the direction of maximum stiffness was more vertically ori-

ented. Several sites in the mandible did not show a consistent direction of maximum stiffness among specimens, although all specimens exhibited significant orthotropy. Mandibular cortical thickness varied significantly ($P < 0.001$) between sites, and decreased from 3.7 mm (SD = 0.9) anteriorly to 1.4 mm posteriorly (SD = 0.1). The cortical plate was also significantly thicker ($P < 0.003$) on the facial side than on the lingual side. Bone was 50–100% stiffer in the longitudinal direction (E_3 , 20–30 GPa) than in the circumferential or tangential directions (E_2 or E_1 ; $P < 0.001$). The results suggest that material properties and directional variations have an important impact on mandibular mechanics. The accuracy of stresses calculated from strains and average material properties varies regionally, depending on variations in the direction of maximum stiffness and anisotropy. Stresses in some parts of the mandible can be more accurately calculated than in other regions. Limited evidence suggests that the orientations and anisotropies of cortical elastic properties correspond with features of cortical bone microstructure, although the relationship with functional stresses and strains is not clear. *Am J Phys Anthropol* 120:252–277, 2003.

© 2003 Wiley-Liss, Inc.

The deficit of information on cortical material properties and on their directional and regional variations in the human mandible creates problems in interpreting the results of experimental and modeling approaches to mandibular function. While limited information exists on material property variability in the cortices of human long bones (Cowin, 1989; Katz and Meunier, 1987; Weiner et al., 1999; Wirtz et al., 2000), less information is available for the craniofacial skeleton. Studies of mandibular cortical material properties (Arendts and Sigolotto, 1990; Ashman and van Buskirk, 1987; Carter, 1989; Dechow et al., 1992, 1993) have small numbers of specimens from limited anatomical regions.

Inadequate information on material properties complicates the interpretation of mandibular finite element models (Kabel et al., 1999; Koriath et al., 1992). Some mandibular finite element models (Kaewsuriyathumrong and Soma, 1993; Meijer et al., 1993) assume that cortical and cancellous bone

is isotropic (material properties do not vary by direction), homogeneous, and linearly elastic (linear relationship between stress and strain is invariant with changes in time and frequency of loading). Other models (Hart et al., 1992; Koriath et al., 1992) incorporate material properties, even though the assumptions about those properties are speculative, including: 1) direction of maximum stiffness, 2) lack

Grant sponsor: VA Dental Research Fellowship; Grant sponsor: NIH; Grant numbers: DE05691, DE07256.

*Correspondence to: Paul C. Dechow, Ph.D., Department of Biomedical Sciences, Baylor College of Dentistry, 3302 Gaston Ave., Dallas, TX 75246. E-mail: pdechow@tambcd.edu

Received 28 June 2001; accepted 29 March 2002.

DOI 10.1002/ajpa.10121
Published online in Wiley InterScience (www.interscience.wiley.com).

of significant variability, and 3) orthotropy of the bone (material properties are similar in each of three mutually perpendicular directions).

Local anisotropy (material properties differ by direction) and regional variations in skeletal material properties can theoretically have pronounced effects on the relationship between stress and strain (Carter, 1978; Cowin and Hart, 1990; Cowin et al., 1991; Ricos et al., 1996). Studies in the human mandible of in vivo (Asundi and Kishen, 2000) and in vitro cortical bone strain (Andersen et al., 1991a,b; Throckmorton et al., 1992; Throckmorton and Dechow, 1994), and in vivo studies using animal models (Bouvier and Hylander, 1996; Endo, 1973; Hylander, 1979a–c, 1984; Hylander et al., 1987; Marks et al., 1997; Teng and Herring, 1996), do not consider the relevance of variations in material properties. An empirical study (Dechow and Hylander, 2000) which used the results of experiments in macaque mandibles (Hylander, 1979b) found that the orthotropy of mandibular cortical bone should be considered in some but not all cases when interpreting the results of strain gage experiments. Whether knowledge of material properties is relevant must be based on prior knowledge of these properties as well as the functions of the skeletal region under study.

Our objective was to determine the extent of material property variation throughout cortical bone of the human adult dentate mandible. Analyses determined the axes of principal stiffness and the relevance of variations in the direction of maximum stiffness, cortical thickness, cortical density, elastic coefficients, anisotropies, elastic moduli, shear moduli, and Poisson's ratios on our understanding mandibular function.

Previous studies (Arendts and Sigolotto, 1990; Ashman and van Buskirk, 1987; Dechow et al., 1992, 1993), with the exception of Carter (1989), use mandibular geometry to suggest principal axes of material stiffness, thus producing potential errors in material property calculations. For instance, Dechow et al. (1993) use the orientation of the inferior border of the mandible as the presumed direction of maximum stiffness (E_3), based on the predominate orientation of osteons. If the true orientation of maximum stiffness is not in that direction, errors result in the calculation of orthotropic elastic moduli from ultrasonic velocities. A theoretical analysis of "off-axis" velocity measurements through cubic specimens predicted errors of 1.3% in elastic moduli and 5.0% in shear moduli for measurements taken at 10° "off-axis." This error exponentially increases to 4% and 18%, respectively, at 20° "off-axis" (Turner and Cowin, 1988). We tested whether the presumed longitudinal orientation of the axis of maximum stiffness along the lower border of the mandibular corpus is a reasonable estimate. Further, we examined how the orientation of maximum stiffness varied among other regions of the mandible, both in average direction and in the amount of variation, and assessed the impact of this variation on modeling

studies or empirical strain gage studies of mandibular mechanics.

MATERIALS AND METHODS

Specimen selection and preparation

Ten frozen human heads from older individuals ranging in age from 48–81 years were selected from anatomical donations to the willed body program at the University of Texas Southwestern Medical School. Mean age was not significantly different between genders. The 7 males averaged 64.3 years (SD = 11.7), and the 3 females averaged 62.0 years (SD = 17.1). All mandibles were from Caucasian donors.

Selection of heads was based on several criteria, including 1) posterior vertical molar support bilaterally; 2) a minimum of 12 mandibular teeth, allowing for missing third molars and two other teeth, either two nonadjacent posterior teeth or adjacent anterior teeth; 3) no documented history of bone disease; and 4) availability of basic demographic and medical data. All heads were unembalmed and frozen, as the freezing process has minimal effects on the elastic properties of bone compared to the larger effects of embalming (Evans, 1973; Zioupos et al., 2000).

Bone specimens were harvested from throughout the surface of the mandible, including 31 adjacent sites on both the facial and lingual cortex (Fig. 1). The sample was complete except for 1) 3 sites in the upper ramus and coronoid process, where there was a confluence of the cortical plates in some mandibles (number 27, 4/10 individuals; number 28, 4/10 individuals; and number 30, 7/10 individuals); and 2) at lingual site 25 near the inferior alveolar foramen, where the cortical plate was extremely thin and insufficient for preparation and measurement (5/10 individuals). Measurements were conducted on 600 specimens.

Bone preparation was carried out using standard universal precautions (e.g., gloves and masks) to prevent transmission of infectious diseases. Sites were marked with a graphite line parallel to the occlusal plane and an arrowhead indicating anterior. Bone was cooled continuously with a water drip during preparation. Bone cylinders were harvested from the left mandibular cortex, using a slow-speed dental handpiece and a 4.0-mm inner-diameter trephine burr (Nobel Pharma). Cancellous bone on the inner surface of the cortical specimens was removed with fine-grain grinding wheels on a Unimat 4 miniature lathe. Samples were stored in a solution which maintains the elastic properties of cortical bone over time, consisting of equal parts ethanol (95%) and isotonic saline (Ashman et al., 1984; Zioupos et al., 2000).

Measurement technique

We verified diameter and measured the cortical thickness of each bone specimen with a Max-Cal

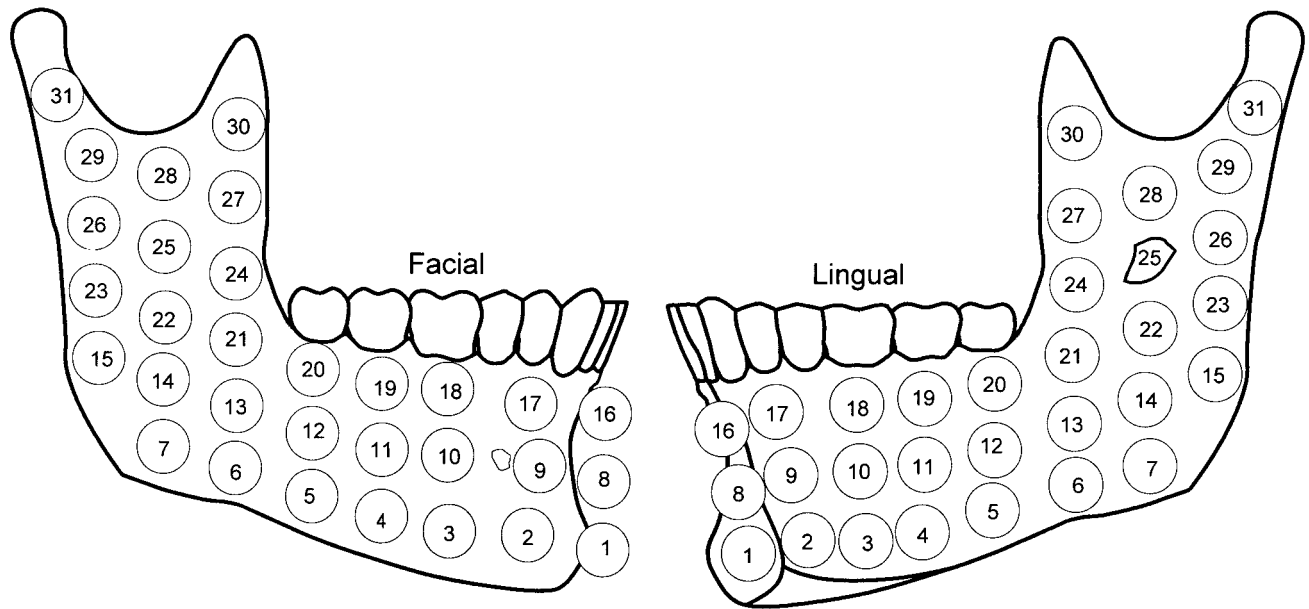


Fig. 1. Thirty-one samples were taken from both the facial and lingual cortices of the human mandible. Samples from sites 1, 8, and 16 were taken from midline at the symphysis.

digital caliper. Cortical thickness was defined as the thickness from periosteum to the cortical-trabecular interface. For ramus sites, trabecular bone was readily visible and removed. For corpus sites, especially at the inferior border, the cortical-trabecular interface was more difficult to define. For these sites, "trabecular" bone was removed endosteally until the cortex had an apparent constant density (or consistent lack of visible porosity). Densities were calculated using Archimedes' buoyancy principle (Ashman et al., 1984) from weight measurements made with a Mettler PM460 analytical balance and densitometry kit.

We measured ultrasonic velocities with a pulse transmission technique (Ashman et al., 1984; Ashman and van Buskirk, 1987; Dechow et al., 1993). Ultrasonic waves were generated with a Hewlett-Packard pulse generator and two sets of mounted piezoelectric transducers (2.25 MHz longitudinal, Panametrics V323-SU, and 5.0 MHz shear, Panametrics V156-RM). Both longitudinal and transverse ultrasonic waves were passed through various axes, including the principal axes (D_2 and D_3) and the cortical thickness (D_1) of each specimen. Time delays were measured using an oscilloscope (Tektronix TDS 420) to make a phase comparison of the signal before and after its transmission through a specimen. Ultrasonic velocities were calculated by dividing the specimen thickness or diameter by the apparent time delay minus the system time delay.

Calculation of elastic coefficients from ultrasonic velocities requires assumptions about the directions of the principal axes of stiffness (D_2 and D_3) prior to preparation of the bone specimen. A cubic or parallelepiped specimen, as used by Ashman et al. (1984), must be prepared so that the principal axes of the

specimen are aligned perpendicular to its faces. This is a problem if these orientations are unknown. As first noted by Carter (1989), collecting cylindrical specimens obviates this problem by allowing the principal axes of stiffness in the plane of the cortical plate to be determined by measuring ultrasonic velocities in multiple orientations around the perimeter of the specimen.

We identified principal axes by measuring longitudinal ultrasonic velocities in 9 orientations in the plane of the cortical plate. We rotated each bone cylinder between the transducer heads for 8 rotations of 22.5° , enabling the orientation of the principal axes to be determined within 11.25° . The graphite line served as the origin for 8 rotations (Fig. 2A). As on a compass, the arrowhead points towards 0° , and was given the directional value of 1. Directions of 45° and 180° were given values of 5 and 9, respectively.

We compared ultrasonic velocities in the directions 1 and 9 (0° and 180° , respectively) as an internal control for measurement reliability. These velocities must be identical, as the two transducers are switched in position relative to the specimen, but the direction of ultrasonic wave propagation is the same. Velocities in the 9 directions were plotted by orientation. The orientation with the highest velocity was the axis of maximum stiffness, as ultrasound passes more rapidly as stiffness increases. The axis of minimum stiffness, or least stiff direction, corresponded to the lowest velocity. These axes were reassigned as D_3 and D_2 , respectively, for the duration of the study (Fig. 2B). In all 600 bone specimens, the axis of minimum stiffness was perpendicular to the axis of maximum stiffness. This relationship validated the assumption of orthotropy, which is a precondition

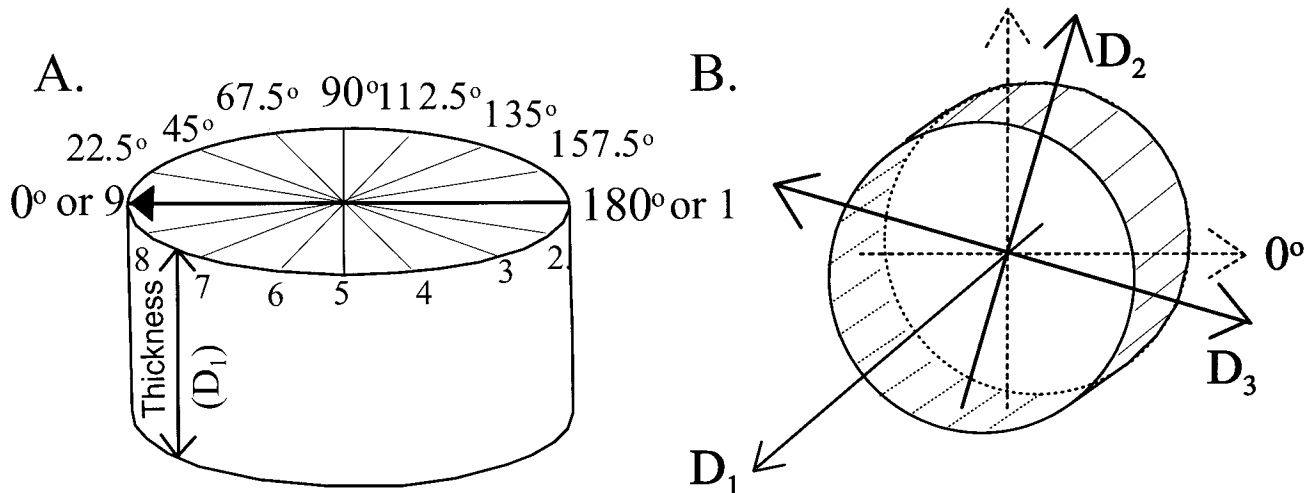


Fig. 2. Bone cylinders represent a cortical plate specimen. Cortical thickness was identified as D_1 . **A:** Arrow parallels occlusal plane. Measurements were taken at angular rotations of 22.5° to determine orientation of principal axes. **B:** Axis of maximum stiffness was identified as D_3 ; axis of minimum stiffness was identified as D_2 . See text for details.

necessary for calculation of elastic properties from ultrasonic velocities (Ashman et al., 1984).

An additional important question is whether reliable ultrasonic velocities can be measured radially in cylindrical specimens. Carter (1989) found that calculated elastic properties from cubic and cylindrical specimens of mandibular cortical bone are similar. We measured both longitudinal and transverse ultrasonic velocities in cubic and cylindrical specimens of aluminum phantoms ($n = 72$) varying from 1.0–12.0 mm on a side or in diameter. We also compared ultrasonic velocities and derived elastic moduli from 40 cubic and 40 cylindrical cortical specimens taken from the symphyseal region of human mandibles. Analysis of variance comparing ultrasonic velocities from different shapes and sizes of aluminum and bone specimens did not reveal any statistically significant differences for specimens under 10.0 mm (Schwartz-Dabney, 2001).

Another concern was the cortical plate thickness in some bone specimens. Ashman et al. (1984) validated the technique for standardized cubes of cortical bone (5 mm on a side), but actually used cortical specimens with thicknesses down to 3 mm. Kohles et al. (1997) validated the technique for measurement of smaller specimens (<1 mm on a side). We tested the effects of changing the thickness of the 4-mm-diameter cylinders to mimic variations in cortical thickness. In mandibular bone, we found that specimens down to a thickness of 1.2 mm could be analyzed with results similar to those obtained from larger or cubic specimens. Specimens with a thickness between 0.6–1.2 mm had increased measurement errors in ultrasonic velocity through D_1 , suggesting a magnification of the effects of inhomogeneities or flaws in the bone matrix for very thin specimens.

In our sample of 600 specimens, 16 (or 2.7%) were thinner than 1.2 mm. In these specimens, accurate

measurements of ultrasonic velocities in the cortical plane (8 measurements per specimen) and densities were collected. To calculate technical constants, we substituted reasonable estimates of three D_1 velocities (1 longitudinal, v_{11} ; and 2 transverse, v_{12} and v_{13}). For each specimen, the estimates were the mean values of v_{11} , v_{12} , and v_{13} from cortical specimens with a thickness of 1.2 mm or greater at the same site on the remaining mandibles. The 16 thin specimens came from 5 of the 10 mandibles, with 5 sites at most coming from one mandible. Likewise, these specimens came from 12 different sites, with 3 specimens at most from any one site. The sites included 3 on the facial side (numbers 7, 17, 30) and 9 on the lingual side (numbers 5, 12–14, 20, 22, 25, and 28). Estimated technical constants were used in ANOVAs with repeated measures, which required complete data sets, but not for the calculations of descriptive statistics.

Elastic properties were calculated from ultrasonic velocities, using a program written in Mathcad. The equations for these calculations were based on mathematical relationships derived from the principles of linear elastic wave theory and Hooke's law (Ashman et al., 1984). Ultrasonic velocities and densities were used to calculate 6×6 matrices, or "C" matrices, including 8 unique elastic coefficients (c_{11} , c_{22} , c_{33} , c_{44} , c_{55} , c_{66} , c_{12} , and c_{23}) and then technical constants (elastic and shear moduli, and Poisson's ratios).

Relationships and definitions for elastic coefficients and the derived material properties are described in detail elsewhere (Ashman et al., 1984; Dechow et al., 1993; van Eijden, 2000). Briefly, Young's modulus or the elastic modulus (E) measures axial stiffness or the amount of deformation (strain) relative to an applied load (stress). Subscripts, as in E_1 , E_2 , or E_3 , indicate the appropriate axis for each elastic modulus. Shear modulus (G)

measures stiffness in shear or angular deformation relative to applied shearing loads in a plane between two axes indicated by the subscripts (G_{12} , G_{31} , or G_{32}). Poisson's ratio (ν) is a measure of stiffness of a structure perpendicular to that of the applied load. It is a ratio of the strain in the secondary direction (response direction) divided by strain in the primary direction (applied load direction). The first subscript indicates the axis of the applied load and the second subscript indicates the response direction as in ν_{12} , ν_{13} , ν_{21} , ν_{23} , ν_{31} , and ν_{32} . We compared relative stiffness between axes by using ratios of elastic coefficients (c_{11}/c_{22} , c_{11}/c_{33} , and c_{22}/c_{33}) and technical constants (E_2/E_3), which are common methods for quantifying anisotropy.

The ratio of the elastic coefficients (c_{22}/c_{33}) or the associated elastic moduli (E_2/E_3) measures the relative differences in stiffness (orthotropy) between the principal axes (D_2 and D_3) in the cortical plane (Kohles et al., 1997; Martin et al., 1998). Stiffness in the direction of D_1 (cortical thickness) to that in the direction of D_2 or D_3 is evaluated by ratios c_{11}/c_{22} and c_{11}/c_{33} , respectively. Anisotropy ratios express the relative homogeneity of an orthotropic material along the two axes under consideration. As ratios approach a value of 1.0, the material is presumed identical in structure along the two axes and isotropic in that plane. As values decline below 1.0, the differences in stiffness by direction are greater, and presumably the organization of the material is more dissimilar between the two perpendicular axes.

Statistical analysis

We used Minitab Statistical Software (release 13.3) for most statistical calculations. However, directions of maximum stiffness, because of their unique circular distribution, required altered methods of calculation (Zar, 1996), which are available in the software program Oriana (Kovach Computing Services, Anglesey, Wales, UK). An additional concern was whether the distribution of orientations was different from a random collection of angles. We used Raleigh's uniformity test (Zar, 1996) to determine whether the means themselves were significant. If angular means were significant, we tested differences between them with a generalization of the Watson-Williams test (Zar, 1996).

The main goal of this investigation was an understanding of variation in cortical material properties throughout the mandible. Descriptive statistics of each variable at each site provided this overview. We were also interested in whether these data showed statistical differences in material properties between regions of the mandible. However, assessment of differences was limited by the sample size of mandibles ($N = 10$). Despite the large number of individual specimens ($N = 600$), ANOVA with a repeated measures design was needed to account for the lack of independence between multiple samples taken from a single mandible (Zar, 1996). We used an unrestricted analysis of variance, with a repeated

measures design and mandible as the random (repeating) factor to test for differences in bone density, cortical thickness, and elastic properties between the two fixed factors of site and side. Because of the low number of mandibles and the large number of possible individual comparisons, we did not attempt post hoc testing of differences between individual sites. F values were used to assess whether on the whole there was a significant difference between the variances within sites and within sides relative to overall variance within sites by mandible, or within sides by mandible, respectively (Minitab User's Guide 2, Release 13, pp. 3-31-3-33, Minitab, Inc., 2000).

Age and gender differences were not the primary concern of this study. However, we attempted to ascertain if there were significant differences in material properties by gender and age within the limited scope of the sample. To determine if there were gender differences, an additional set of ANOVAs, similar to those described above, were conducted in which gender was included as a between-subjects factor. To look for age-related effects, correlation coefficients and plots were generated between age and mean material properties, which were calculated by averaging all values for all sites in each mandible.

Analysis of effects of material property variation on stresses calculated from bone strains

To determine the effects of using *mean* material property values to assess loading patterns in *individuals*, we looked at how individual variations in material property anisotropies and orientations affect the calculation of stress magnitudes and orientations from strains. We used 5 representative specimens (Table 1) that covered the majority of the demonstrated range of E_2/E_3 anisotropy (0.5–0.9) in the 600 samples. We determined the effects of these anisotropies over the possible range of angles between the maximum principal strains and principal axis orientations (Δpa) on 2 parameters: 1) the ratios of minimum to maximum strains (ϵ_q/ϵ_p) compared to the ratios of minimum to maximum stresses (σ_q/σ_p), and 2) the differences in the angles between the maximum principal strains and maximum principal stresses ($\Delta\Phi$) (Dechow and Hylander, 2000; Dechow et al., 1993).

We calculated $\Delta\Phi$ and σ_q/σ_p , if ϵ_q/ϵ_p was held constant at 1.0, while anisotropy ranged from 0.5–0.9 and Δpa ranged from 0–90°. The ϵ_q/ϵ_p value of 1.0 was used, as it is near the average result from in vivo strain gage measurements of macaque mandibles (Dechow and Hylander, 2000: $\epsilon_q/\epsilon_p = 1.1$; Daegling and Hylander, 1998: $\epsilon_q/\epsilon_p = 0.98$).

We also calculated $\Delta\Phi$ and σ_q/σ_p for Δpa of 0°, 25°, 45°, 65°, and 90° when ϵ_q/ϵ_p ranged from 0.5–3.0 (similar to the range found in macaque mandibles). The material properties used during these calculations were from the representative specimen (Table

TABLE 1. Material properties of five mandibular samples of varying anisotropy¹

St	Sd	Area	E ₂	E ₃	G ₂₃	ν ₂₃	ν ₃₂	E ₂ /E ₃
18	L	Alv	12.7	25.2	6.8	0.20	0.41	0.5
3	F	Infbor	13.6	22.5	7.3	0.22	0.37	0.6
5	F	Infbor	16.0	23.0	7.2	0.24	0.34	0.7
1	L	Sym	16.8	21.1	7.4	0.32	0.41	0.8
11	L	Midbod	20.6	22.9	6.8	0.27	0.30	0.9

¹ St, site; Sd, side; F, facial; L, lingual; Sym, symphysis; Infbor, inferior border; Midbod, midbody. Elastic and shear moduli are in GPa.

1) in which $E_2/E_3 = 0.6$ (where near maximum σ_q/σ_p errors occurred).

We determined the magnitude of potential errors regionally when stresses were calculated from strains and $\epsilon_q/\epsilon_p = 1.0$. For each of the 62 sites, maximum errors at the 95th percentile of the sample variance were computed from variance in principal axis orientation and E_2/E_3 anisotropy. For example, at facial site number 5 along the inferior border of the corpus, 95% of individuals had a principal axis orientation within 56° of the mean and an E_2/E_3 anisotropy greater than 0.85. Within this 95% limit, calculated σ_q/σ_p deviated up to 19% from the actual mean.

RESULTS

Direction of maximum stiffness

The direction of maximum stiffness varied significantly among sites ($F = 15.1$, $P < 0.001$) (Fig. 3A). Several sites (gray in Fig. 3A) had no significant orientation according to the Raleigh uniformity test ($P > 0.05$). An example of the range of variation for oriented and nonoriented sites is given in Figure 4.

All sites exhibited variation in the direction of maximum stiffness (Table 2). Sites with the least variation were found at the inferior corpus and the posterior ramus on both cortices and mid-ramus on the facial cortex. Variation was greater near the coronoid and condylar processes, the sigmoid notch area, midbody for both cortices, and at the facial alveolar process. Nonoriented sites were found within the submandibular fossa, masseteric insertion, and symphyseal alveolar process (Fig. 3).

The direction of maximum stiffness had consistent differences in orientation between the body and the ramus, and between the facial and lingual cortices. Anterior to the second molar on the facial and lingual cortices, the mean orientation was near the occlusal plane, ranging from -9.0° ($SD = 11.1^\circ$) to 39.9° ($SD = 22.0^\circ$). In the facial ramus, the orientation was more vertical, ranging from 54.0° ($SD = 11.1^\circ$) mid-ramus to 98.9° ($SD = 18.0^\circ$) at the coronoid process. In the lingual ramus, orientations were less vertical, ranging from 18.3° ($SD = 13.3^\circ$) at the inferior border to 81.7° ($SD = 28.2^\circ$) near the coronoid process.

Cortical thickness

We found significant differences in thickness among the facial and lingual cortices (sides) ($F = 16.3$, $P < 0.003$) and among sites ($F = 10.1$, $P <$

0.001) (Fig. 3B, Table 2). Cortical bone was thicker in the corpus than in the ramus, and thicker in the facial than in the lingual corpus. Overall, the cortex was thickest at the lower border of the symphysis.

Density

Cortical density differed among sites ($F = 5.5$, $P < 0.001$) but not sides (Fig. 3C, Table 2). Variability in the mean density throughout most sites was small, ranging between 1,850–2,000 mg/cm³. The exception was the lower density in several symphyseal sites.

Elastic moduli

Elastic coefficients (c_{11} , c_{22} , and c_{33}) (Table 3) showed similar patterns of variation as the elastic moduli (E_1 , E_2 , and E_3), where in each specimen $E_3 > E_2 > E_1$ (Fig. 5, Table 4). The grand mean elastic moduli of all 600 specimens were 22.8 GPa ($SD = 5.4$) for E_3 , 17.9 GPa ($SD = 2.5$) for E_2 , and 12.7 GPa ($SD = 1.8$) for E_1 .

E_1 differed among sites ($F = 2.4$, $P < 0.001$) but not sides. The differences among sites were less than for E_2 and E_3 , and most sites showed consistent values for E_1 . Other than 5 sites within the facial ramus, all sites had moduli less than 13.9 GPa.

E_2 differed among sites ($F = 5.7$, $P < 0.001$) but not sides. E_2 moduli were consistently larger in the ramus, where they were on average about 20% greater than in the mandibular body.

E_3 differed among sites ($F = 4.4$, $P < 0.001$) and sides ($F = 6.0$, $P = 0.03$). E_3 was larger on the facial cortex in 26 of 31 sites. On both cortices, E_3 moduli were larger in the ramus than in the corpus.

Anisometry

All specimens had a similar pattern between the elastic coefficients and the corresponding elastic moduli, where $c_{11} < c_{22} < c_{33}$ and $E_1 < E_2 < E_3$ (Tables 2–4, Figs. 5, 6). Note that smaller values of anisometry ratios indicated increased anisotropy.

c_{11}/c_{22} differed among sites ($F = 5.5$, $P < 0.001$) but not sides. On the facial cortex, sites with the greatest anisotropy were located in the ramus. The lingual cortex had a region of greater anisotropy through the midbody and angle. This pattern had parallels with the distribution of E_2 because c_{22} (or E_2) was more variable than c_{11} (or E_1), and thus anisotropy was usually greatest where c_{22} (or E_2) had the largest values.

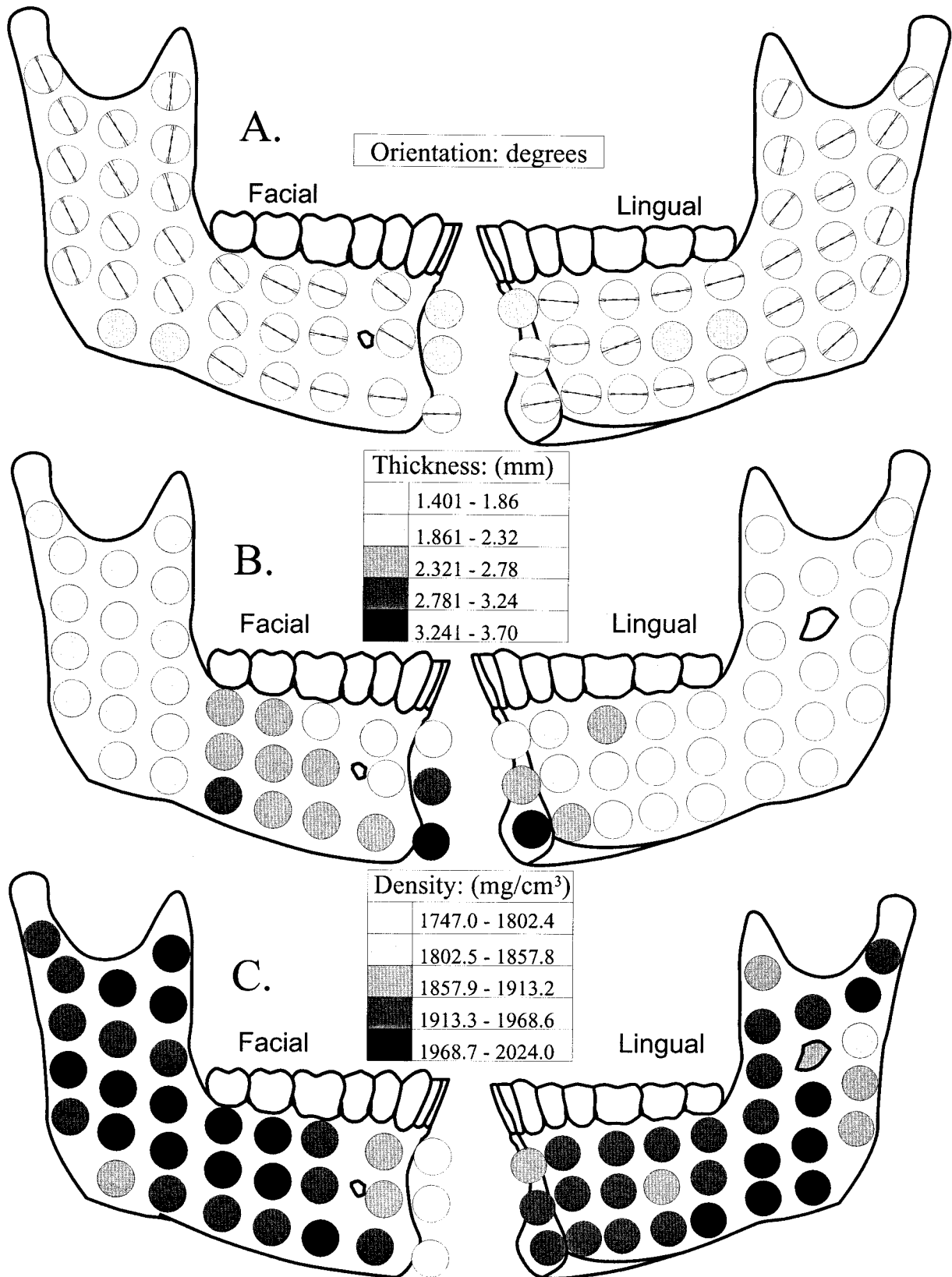


Fig. 3. Cortical plate principal axis orientation, thickness, and density for sites in human dentate mandibles. **A:** Solid bars indicate the axes of maximum stiffness. Dashed bars represent 95% confidence intervals. Gray sites had no significant orientation. **B:** Thickness (mm). The cortex was thickest at the inferior symphysis and thinnest throughout the lingual ramus. **C:** Density (mg/cm^3). There was more variation in density on the facial cortex. See text for details.

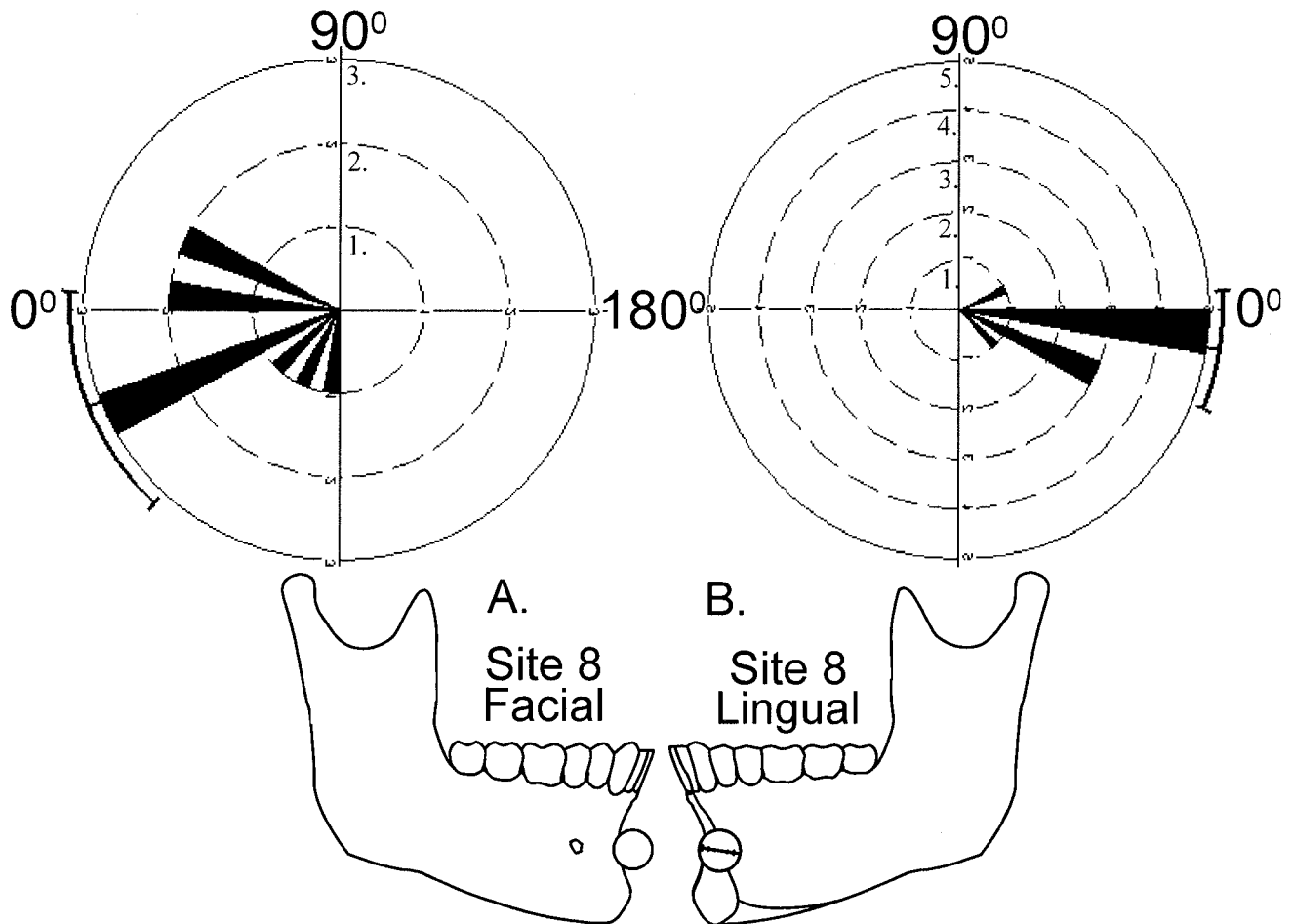


Fig. 4. Examples of circular statistics. Unidirectional rays along the appropriate 22.5° increment represent individual specimen orientation. Each circular ring encloses a specimen ($N = 1$ in each appropriate orientation), and rays increase in magnitude to represent total number of specimens with that orientation. Facial site 8 (A) had no significant orientation, with only 3 modal specimens at 22.5° and the other 7 specimens spread over 112.5° (within 67.5°). Lingual site 8 (B) had a strong principal orientation at -8.9° , with 5 specimens oriented at 0° and the other 5 specimens within 45° .

c_{11}/c_{33} differed among sites ($F = 4.1, P < 0.001$) and sides ($F = 6.5, P = 0.03$). Values were slightly less anisotropic lingually in a number of sites, including at the symphysis, the alveolar process below the molars, the coronoid process, and below the sigmoid notch, and facially at the symphyseal alveolar process.

c_{22}/c_{33} differed among sites ($F = 5.0, P < 0.001$) and sides ($F = 8.7, P = 0.02$). The facial cortex had equal or greater anisotropy compared to the lingual cortex at most sites (Fig. 6), with four exceptions (sites 7, 16, 24, and 28). These sites were found at the masseteric insertion and the ramus beneath the coronoid process and the sigmoid notch. Decreased anisotropy was found in cortical bone at the symphysis, particularly in the alveolar process, lingual midbody, and angle regions.

Shear moduli

Overall, shear moduli were not significantly different between facial and lingual sides of the mandible, but each had significant differences among sites (G_{12} :

$F = 1.7, P = 0.02$; G_{31} : $F = 2.0, P = 0.002$; G_{23} : $F = 5.7, P < 0.001$). In each specimen, $G_{23} > G_{31} > G_{12}$ (Fig. 7, Table 4). The grand means of the shear moduli were 7.4 GPa (SD = 0.8) for G_{23} , 5.5 GPa (SD = 0.7) for G_{31} , and 5.0 GPa (SD = 0.6) for G_{12} .

G_{12} had slightly different patterns of moduli on the facial and lingual cortices. The lingual cortex had larger moduli at the inferior border of the symphysis. The facial cortex had larger moduli at the posterior border and condylar neck. Otherwise, facial and lingual cortices were similar, with larger moduli at the alveolar process beneath the molars, the coronoid process, and some sites in mid-ramus.

At most sites, G_{31} was similar between adjacent facial and lingual cortices. G_{31} was least at the symphysis, especially on the facial side. The largest values were found facially near or below the most posterior molar.

In G_{23} , regional cortical patterns were more prominent. Within the facial cortex, G_{23} was smaller anterior to the mental foramen, at the condylar neck, and at the angle. Within the lin-

TABLE 2. Principal axis, thickness, density, and anisotropy for human dentate mandibles¹

St	Sd	Area	Principal axis (degrees)		Thickness (mm)		Density (mg/cm ³)		Anisotropy (c ₂₂ /c ₃₃)		Anisotropy (c ₁₁ /c ₂₂)		Anisotropy (c ₁₁ /c ₃₃)		Anisotropy (E ₂ /E ₃)	
			Mean	SD	Mean	SD	Mean	SD	Mean	SD	Mean	SD	Mean	SD	Mean	SD
1	F	Sym	0.0	14.3	3.3	1.3	1,764	154	0.67	0.09	0.86	0.11	0.57	0.06	0.69	0.13
2	F	Sym	4.5	13.5	2.6	0.4	1,917	110	0.63	0.06	0.81	0.06	0.51	0.05	0.76	0.12
3	F	Infbor	13.5	11.1	2.4	0.3	1,975	100	0.63	0.04	0.81	0.05	0.51	0.04	0.73	0.10
4	F	Infbor	24.7	12.1	2.6	0.3	1,955	132	0.64	0.06	0.78	0.05	0.50	0.06	0.73	0.09
5	F	Infbor	32.2	24.1	2.8	0.4	1,937	96	0.71	0.06	0.74	0.07	0.52	0.07	0.86	0.12
6	F	Angle	*	35.2	2.2	0.4	1,947	46	0.69	0.08	0.75	0.05	0.52	0.05	0.93	0.18
7	F	Angle	*	35.5	2.0	0.7	1,866	141	0.78	0.10	0.69	0.07	0.53	0.08	0.92	0.19
8	F	Sym	*	35.2	2.9	0.8	1,747	151	0.72	0.05	0.76	0.08	0.55	0.06	0.82	0.10
9	F	Sym	31.3	14.9	1.9	0.4	1,909	44	0.63	0.08	0.82	0.07	0.52	0.05	0.76	0.14
10	F	Midbod	9.5	22.8	2.5	1.2	1,955	159	0.73	0.08	0.75	0.07	0.55	0.06	0.93	0.21
11	F	Midbod	31.3	14.9	2.7	0.8	2,009	64	0.67	0.06	0.82	0.08	0.55	0.04	0.81	0.17
12	F	Midbod	49.5	13.5	2.5	0.5	1,974	43	0.72	0.07	0.78	0.06	0.56	0.05	0.82	0.16
13	F	Midram	60.8	10.3	1.9	0.4	1,979	73	0.71	0.03	0.76	0.05	0.54	0.05	0.77	0.11
14	F	Angle	58.5	11.1	2.0	0.4	2,017	85	0.68	0.04	0.75	0.07	0.51	0.07	0.71	0.13
15	F	Posbor	67.5	14.3	1.9	0.3	1,922	109	0.66	0.04	0.82	0.05	0.54	0.04	0.69	0.09
16	F	Sym	*	34.8	2.2	0.7	1,698	110	0.77	0.09	0.81	0.10	0.63	0.11	0.83	0.16
17	F	Sym	39.9	22.0	2.0	0.9	1,869	88	0.73	0.07	0.78	0.09	0.57	0.10	0.89	0.20
18	F	Alv	20.2	15.8	2.3	0.5	1,964	109	0.73	0.07	0.77	0.06	0.56	0.09	0.86	0.11
19	F	Alv	26.8	19.6	2.5	0.4	1,977	76	0.69	0.05	0.83	0.05	0.57	0.05	0.78	0.16
20	F	Alv	44.0	25.2	2.7	0.5	2,003	96	0.67	0.07	0.81	0.04	0.54	0.05	0.74	0.16
21	F	Midram	56.3	11.3	1.9	0.3	2,024	65	0.72	0.10	0.72	0.09	0.52	0.06	0.76	0.18
22	F	Midram	54.0	11.1	1.7	0.2	1,975	67	0.67	0.06	0.76	0.06	0.51	0.04	0.81	0.12
23	F	Posbor	63.0	13.5	2.1	0.6	1,998	113	0.66	0.04	0.78	0.05	0.52	0.04	0.72	0.14
24	F	Midram	70.2	21.2	2.3	0.5	1,958	63	0.77	0.05	0.74	0.05	0.57	0.06	0.88	0.17
25	F	Midram	55.0	33.3	1.9	0.3	1,945	60	0.72	0.05	0.72	0.05	0.52	0.03	0.86	0.17
26	F	Posbor	60.8	10.3	2.2	0.3	1,963	76	0.69	0.06	0.79	0.06	0.54	0.03	0.76	0.19
27	F	Cor	98.9	18.0	2.3	0.9	2,006	95	0.71	0.08	0.74	0.07	0.52	0.03	0.76	0.16
28	F	Midram	56.4	20.8	2.1	0.8	1,978	52	0.76	0.07	0.71	0.10	0.54	0.07	0.98	0.15
29	F	Cond	60.7	14.4	2.2	0.4	1,958	75	0.65	0.04	0.80	0.05	0.51	0.04	0.69	0.13
30	F	Cor	93.5	26.9	2.0	0.6	2,002	80	0.66	0.05	0.78	0.11	0.51	0.08	0.65	0.12
31	F	Cond	65.3	12.1	1.9	0.2	1,924	59	0.66	0.04	0.78	0.05	0.52	0.04	0.74	0.11
1	L	Sym	10.9	18.2	3.7	0.9	1,938	55	0.72	0.07	0.84	0.10	0.60	0.06	0.94	0.21
2	L	Sym	-9.0	11.1	3.0	0.8	1,948	101	0.69	0.04	0.84	0.08	0.58	0.04	0.83	0.16
3	L	Infbor	0.0	10.0	2.2	0.7	1,967	81	0.68	0.05	0.83	0.09	0.56	0.05	0.80	0.13
4	L	Infbor	9.0	11.1	1.8	0.5	1,964	115	0.69	0.06	0.77	0.06	0.53	0.05	0.85	0.09
5	L	Infbor	18.0	13.5	1.8	0.5	2,013	56	0.74	0.05	0.75	0.07	0.55	0.04	0.92	0.11
6	L	Angle	18.3	13.3	1.8	0.4	1,980	109	0.77	0.11	0.71	0.09	0.54	0.08	0.91	0.23
7	L	Angle	46.0	22.9	1.7	0.3	1,970	63	0.71	0.07	0.76	0.07	0.54	0.05	0.85	0.17
8	L	Sym	-8.9	18.0	2.6	0.8	1,946	56	0.73	0.08	0.81	0.07	0.59	0.04	0.84	0.21
9	L	Sym	4.5	13.5	2.1	0.3	1,967	61	0.69	0.04	0.80	0.06	0.55	0.04	0.83	0.16
10	L	Midbod	22.1	28.8	2.0	0.4	1,957	49	0.78	0.08	0.72	0.08	0.56	0.07	0.97	0.18
11	L	Midbod	*	32.7	1.8	0.4	1,902	131	0.79	0.06	0.73	0.05	0.58	0.05	0.99	0.12
12	L	Midbod	*	36.3	1.4	0.4	1,941	110	0.74	0.11	0.73	0.07	0.55	0.08	0.96	0.14
13	L	Midram	23.9	24.0	1.4	0.3	1,972	56	0.81	0.09	0.72	0.06	0.57	0.05	0.99	0.17
14	L	Angle	38.5	29.6	1.5	0.3	1,992	119	0.74	0.10	0.68	0.04	0.50	0.06	0.85	0.25
15	L	Posbor	60.6	17.7	1.7	0.4	1,874	88	0.65	0.05	0.74	0.10	0.49	0.07	0.66	0.13
16	L	Sym	*	36.6	1.7	0.2	1,867	89	0.79	0.07	0.75	0.07	0.59	0.07	0.94	0.16
17	L	Sym	-4.4	9.0	2.1	0.5	1,958	38	0.69	0.07	0.79	0.07	0.54	0.05	0.82	0.16
18	L	Alv	2.2	12.1	2.3	0.6	1,916	48	0.72	0.08	0.87	0.10	0.62	0.08	0.78	0.16
19	L	Alv	9.1	15.0	1.8	0.5	1,931	82	0.71	0.07	0.84	0.11	0.59	0.11	0.82	0.10
20	L	Alv	15.8	10.3	1.7	0.4	1,916	72	0.75	0.07	0.80	0.06	0.60	0.07	0.89	0.16
21	L	Midram	31.4	18.0	1.8	0.4	1,966	93	0.72	0.10	0.73	0.08	0.53	0.07	0.87	0.19
22	L	Midram	29.1	17.6	1.4	0.3	1,980	89	0.74	0.10	0.72	0.08	0.54	0.07	0.90	0.18
23	L	Posbor	67.5	10.0	1.5	0.2	1,892	102	0.69	0.09	0.73	0.09	0.50	0.05	0.73	0.18
24	L	Midram	51.8	14.4	2.0	0.3	1,922	116	0.70	0.04	0.76	0.07	0.53	0.05	0.78	0.16
25	L	Midram	27.1	16.9	1.5	0.5	1,895	138	0.69	0.05	0.73	0.04	0.50	0.03	0.79	0.18
26	L	Posbor	51.8	14.4	1.5	0.3	1,853	135	0.67	0.04	0.80	0.08	0.54	0.05	0.72	0.10
27	L	Cor	81.7	28.2	1.9	0.3	1,941	66	0.69	0.06	0.74	0.07	0.50	0.02	0.76	0.11
28	L	Midram	33.4	25.4	1.7	0.6	1,959	142	0.68	0.06	0.87	0.07	0.59	0.05	0.71	0.12
29	L	Cond	59.2	29.8	1.7	0.2	1,988	72	0.65	0.04	0.77	0.07	0.50	0.05	0.70	0.12
30	L	Cor	75.4	21.4	1.4	0.1	1,902	53	0.66	0.13	0.89	0.15	0.57	0.02	0.68	0.25
31	L	Cond	40.5	13.6	1.8	0.2	1,926	85	0.69	0.07	0.76	0.04	0.53	0.07	0.83	0.16

¹ St, site; Sd, side; F, facial; L, lingual; Sym, symphysis; Infbor, inferior border; Midbody, midbody; Alv, alveolar process; Cor, coronoid process; Cond, condylar process; Midram, middle of ramus; Posbor, posterior border.

* No significant orientation within a site. See text for description.

gual cortex, moduli were smaller at the symphysis, at the condylar neck, in the alveolar and midbody regions inferior to the molars, and in the mid-ramus region.

Poisson's ratio

Poisson's ratios were not significantly different between facial and lingual sides, although each had

TABLE 3. Elastic coefficients (in GPa) for human dentate mandibles¹

St	Sd	Area	C ₁₁		C ₂₂		C ₃₃		C ₄₄		C ₅₅		C ₆₆		C ₁₂		C ₂₃	
			Mean	SD	Mean	SD	Mean	SD	Mean	SD	Mean	SD	Mean	SD	Mean	SD	Mean	SD
1	F	Sym	17.3	2.5	20.2	2.0	30.5	4.7	6.3	0.8	4.7	0.5	4.4	0.9	8.4	1.8	10.4	3.4
2	F	Sym	18.7	2.2	23.0	2.4	36.6	3.3	7.2	0.7	5.2	0.7	4.7	0.6	9.3	2.6	14.9	2.9
3	F	Infbor	19.1	2.6	23.7	3.3	37.5	4.5	7.7	0.8	5.5	0.8	4.9	0.9	9.4	3.2	14.8	2.7
4	F	Infbor	19.2	3.0	24.5	3.3	38.2	2.7	7.8	0.9	5.6	0.7	5.0	0.5	9.2	3.5	14.0	2.8
5	F	Infbor	18.4	2.9	24.9	3.5	35.0	2.3	7.6	0.8	5.6	0.6	4.9	0.3	8.5	3.2	13.8	3.6
6	F	Angle	18.7	2.1	25.2	2.9	36.4	2.4	7.6	0.3	5.2	0.4	4.8	0.4	9.2	2.3	16.4	2.7
7	F	Angle	16.2	2.5	23.7	3.9	30.6	3.8	6.9	0.7	5.0	0.2	4.6	0.4	7.0	2.6	10.9	3.4
8	F	Sym	15.8	2.4	20.8	3.1	28.9	4.9	6.4	0.8	4.8	0.6	4.3	0.5	7.2	1.7	10.5	3.8
9	F	Sym	18.0	2.1	21.9	2.0	35.0	3.9	7.2	0.9	5.2	0.6	4.6	0.4	8.9	1.7	14.9	3.7
10	F	Midbod	19.2	3.6	25.6	4.4	35.1	4.7	7.4	1.3	5.4	0.9	4.8	0.5	9.7	2.8	15.1	3.5
11	F	Midbod	20.8	2.2	25.6	3.7	37.8	2.8	7.6	0.6	5.8	0.5	5.1	0.5	10.5	2.5	15.7	4.5
12	F	Midbod	19.9	2.0	25.7	2.6	35.7	1.5	7.9	0.5	5.8	0.7	5.3	0.7	9.3	2.6	13.3	3.3
13	F	Midram	19.5	2.1	25.7	2.3	36.5	3.2	7.8	0.6	5.9	0.5	5.0	0.3	9.5	2.2	12.9	2.3
14	F	Angle	18.8	2.5	25.1	2.9	37.0	3.7	7.9	0.3	5.8	0.7	5.2	0.8	8.4	2.4	10.8	3.9
15	F	Posbor	18.7	1.4	23.0	2.0	34.9	4.0	7.4	0.7	5.5	0.7	4.8	0.5	9.1	1.8	11.7	3.4
16	F	Sym	14.9	1.7	18.7	3.2	24.3	4.3	5.7	0.7	4.7	0.6	4.5	0.7	6.0	2.1	7.9	2.5
17	F	Sym	17.5	1.8	22.5	2.0	30.9	3.3	6.6	0.7	5.3	0.8	4.9	0.9	7.8	2.8	12.5	3.3
18	F	Alv	19.3	2.8	25.2	2.9	34.7	5.1	7.5	0.7	5.4	0.5	5.2	0.6	8.9	2.4	13.6	2.8
19	F	Alv	20.7	2.6	24.8	2.0	36.1	3.0	7.6	0.6	5.8	0.7	5.3	0.7	10.1	2.6	13.7	3.1
20	F	Alv	20.4	2.7	25.2	2.7	37.9	5.7	7.9	1.0	5.9	0.8	5.4	0.7	9.7	2.6	13.3	4.0
21	F	Midram	19.4	2.6	27.0	3.3	37.6	2.7	8.2	0.6	5.8	0.5	5.1	0.6	9.1	2.8	12.7	3.9
22	F	Midram	18.8	2.1	24.7	2.2	36.9	3.4	7.8	0.8	5.7	0.9	5.3	0.8	8.2	2.1	13.9	1.9
23	F	Posbor	19.1	2.5	24.4	2.7	37.1	4.4	7.8	0.7	5.6	0.4	5.4	0.7	8.4	2.6	11.8	2.7
24	F	Midram	19.1	1.7	26.1	1.7	33.9	2.4	7.7	0.5	5.4	0.7	4.9	0.6	9.3	2.0	13.0	2.8
25	F	Midram	18.6	1.8	25.8	2.2	35.9	3.0	7.6	0.7	5.6	0.5	5.2	0.5	8.2	2.1	13.0	3.2
26	F	Posbor	19.5	2.1	24.8	2.5	36.0	2.9	7.6	0.7	5.5	0.5	5.2	0.4	9.1	2.3	11.9	3.9
27	F	Cor	18.7	2.2	25.5	2.5	35.9	4.1	7.8	0.7	5.7	0.4	5.2	0.6	8.4	2.2	11.1	2.6
28	F	Midram	18.8	3.6	26.3	2.2	34.7	2.6	7.7	0.7	5.5	0.7	5.0	0.5	8.9	3.7	14.2	4.5
29	F	Cond	18.9	2.3	23.8	2.2	36.8	3.0	7.7	0.5	5.5	0.3	4.9	0.6	9.1	2.7	12.0	3.9
30	F	Cor	18.2	3.1	23.4	1.9	35.8	3.5	7.5	0.7	5.8	0.7	5.2	0.4	7.8	2.9	8.6	2.5
31	F	Cond	17.8	2.3	22.8	2.2	34.3	2.3	7.2	0.4	5.6	0.7	5.2	0.6	7.3	2.3	10.2	3.4
1	L	Sym	20.3	2.6	24.4	2.6	34.1	3.1	7.1	1.0	5.9	0.8	5.2	0.6	9.9	2.3	15.2	3.3
2	L	Sym	20.4	2.5	24.5	2.6	35.4	3.8	7.6	0.8	6.0	0.7	5.2	0.7	10.0	2.0	14.8	3.8
3	L	Infbor	19.9	1.7	24.3	3.1	35.9	4.8	7.6	0.9	5.7	0.4	5.1	0.6	9.7	1.6	14.4	3.4
4	L	Infbor	19.1	2.8	24.7	3.0	35.9	4.8	7.5	0.8	5.5	0.8	5.0	0.7	9.1	1.7	14.9	3.9
5	L	Infbor	19.9	1.9	26.5	1.6	35.8	2.5	7.8	0.6	5.4	0.6	5.0	0.6	9.9	1.6	15.7	2.3
6	L	Angle	19.0	3.4	26.9	4.0	35.1	3.1	8.0	0.7	5.5	0.6	5.0	0.6	9.1	3.0	13.6	2.8
7	L	Angle	18.6	1.7	24.8	3.2	34.8	3.0	7.5	0.8	5.4	0.6	5.1	0.5	8.5	1.9	13.6	2.2
8	L	Sym	20.2	2.0	24.9	2.0	34.4	2.9	7.2	0.8	5.7	0.5	5.0	0.5	10.2	2.4	14.0	2.5
9	L	Sym	19.9	1.9	24.9	0.9	36.0	2.0	7.6	0.7	5.7	0.4	5.3	0.4	9.3	2.2	14.1	3.6
10	L	Midbod	19.0	2.5	26.4	2.9	33.9	2.8	7.6	0.8	5.5	0.5	4.9	0.3	9.2	2.2	14.5	2.7
11	L	Midbod	17.8	3.0	24.4	3.8	30.9	4.0	7.0	0.8	5.4	0.6	5.0	0.5	7.8	2.5	13.4	3.0
12	L	Midbod	17.4	2.5	23.9	3.4	32.2	3.0	7.1	0.8	5.0	0.6	5.1	0.7	7.3	2.2	13.3	1.9
13	L	Midram	18.2	1.3	25.6	2.0	31.9	2.5	7.4	0.6	5.1	0.7	5.1	0.6	8.0	1.6	13.0	1.7
14	L	Angle	17.8	2.1	26.4	3.7	35.7	1.8	8.1	0.4	5.8	1.1	5.0	0.5	7.8	2.3	11.0	4.9
15	L	Posbor	16.3	3.2	22.0	3.6	33.6	4.4	6.7	0.6	5.2	0.5	4.5	0.5	7.3	3.8	9.1	3.8
16	L	Sym	17.6	2.4	23.4	2.3	29.8	2.1	6.5	0.4	5.1	0.6	4.9	0.6	7.9	2.0	11.9	2.9
17	L	Sym	19.3	1.5	24.5	2.4	35.8	2.7	7.5	0.6	5.5	0.7	4.9	0.6	9.6	1.9	14.4	2.6
18	L	Alv	19.9	1.9	22.9	2.0	32.1	3.1	6.9	0.5	5.5	0.4	5.2	0.7	9.5	2.6	12.7	2.3
19	L	Alv	19.0	3.0	22.6	1.5	32.2	2.0	6.8	0.6	5.3	0.5	5.2	0.6	8.6	3.0	12.9	3.9
20	L	Alv	18.7	2.2	23.5	2.4	31.5	2.5	6.8	0.6	5.5	0.6	5.1	0.7	8.6	1.5	12.9	2.3
21	L	Midram	18.2	2.9	25.0	3.5	34.6	2.4	7.5	0.7	5.6	0.6	5.0	0.6	8.2	2.4	13.3	2.6
22	L	Midram	17.2	2.2	24.0	3.5	32.4	4.3	7.3	0.8	5.4	0.7	5.3	1.0	6.6	1.6	11.7	2.8
23	L	Posbor	16.2	2.2	22.4	3.2	32.3	2.8	6.9	0.7	5.2	0.6	4.9	0.5	6.5	1.7	8.7	4.2
24	L	Midram	17.8	2.3	23.5	2.4	33.7	2.8	7.3	0.7	5.3	0.6	5.0	0.8	7.9	2.6	11.3	3.3
25	L	Midram	15.9	1.6	21.8	2.4	31.6	2.3	6.9	1.0	5.2	0.6	4.8	0.4	6.3	1.6	9.5	3.3
26	L	Posbor	17.1	1.9	21.4	3.2	31.7	4.5	6.8	0.8	5.0	1.0	4.7	0.7	7.7	1.3	10.5	3.1
27	L	Cor	16.7	2.0	22.8	1.6	33.4	3.5	7.4	0.5	5.1	0.7	5.0	0.2	6.8	2.2	10.2	3.6
28	L	Midram	18.9	2.1	21.9	4.0	32.3	4.9	7.0	1.1	5.5	0.7	5.0	0.4	9.0	1.6	11.1	5.0
29	L	Cond	18.3	2.3	23.7	2.2	36.6	2.2	7.5	0.7	5.3	0.5	5.0	0.5	8.4	2.3	11.7	4.0
30	L	Cor	17.9	3.3	20.3	2.4	31.4	6.3	6.8	1.3	5.7	1.0	5.4	0.6	7.2	3.3	7.6	3.8
31	L	Cond	17.5	2.3	22.9	2.7	33.2	2.1	7.1	0.5	5.4	0.7	5.1	0.8	7.3	2.1	12.4	3.5

¹ See Table 2 for abbreviations.

significant differences among sites (ν_{12} : $F = 2.3, P < 0.001$; ν_{13} : $F = 3.9, P < 0.001$; ν_{21} : $F = 1.9, P = 0.004$; ν_{23} : $F = 3.5, P < 0.001$; ν_{31} : $F = 3.4, P < 0.001$; ν_{32} : $F = 3.8, P < 0.001$). Grand means for Poisson's ratios were 0.18 (SD = 0.11) for ν_{12} , 0.31 (SD = 0.10)

for ν_{13} , 0.25 (SD = 0.13) for ν_{21} , 0.28 (SD = 0.10) for ν_{23} , 0.53 (SD = 0.13) for ν_{31} , and 0.34 (SD = 0.08) for ν_{32} (Fig. 8, Table 5).

Due to shared symmetry, patterns for ν_{12} and ν_{21} have similarities. However, since the elastic moduli

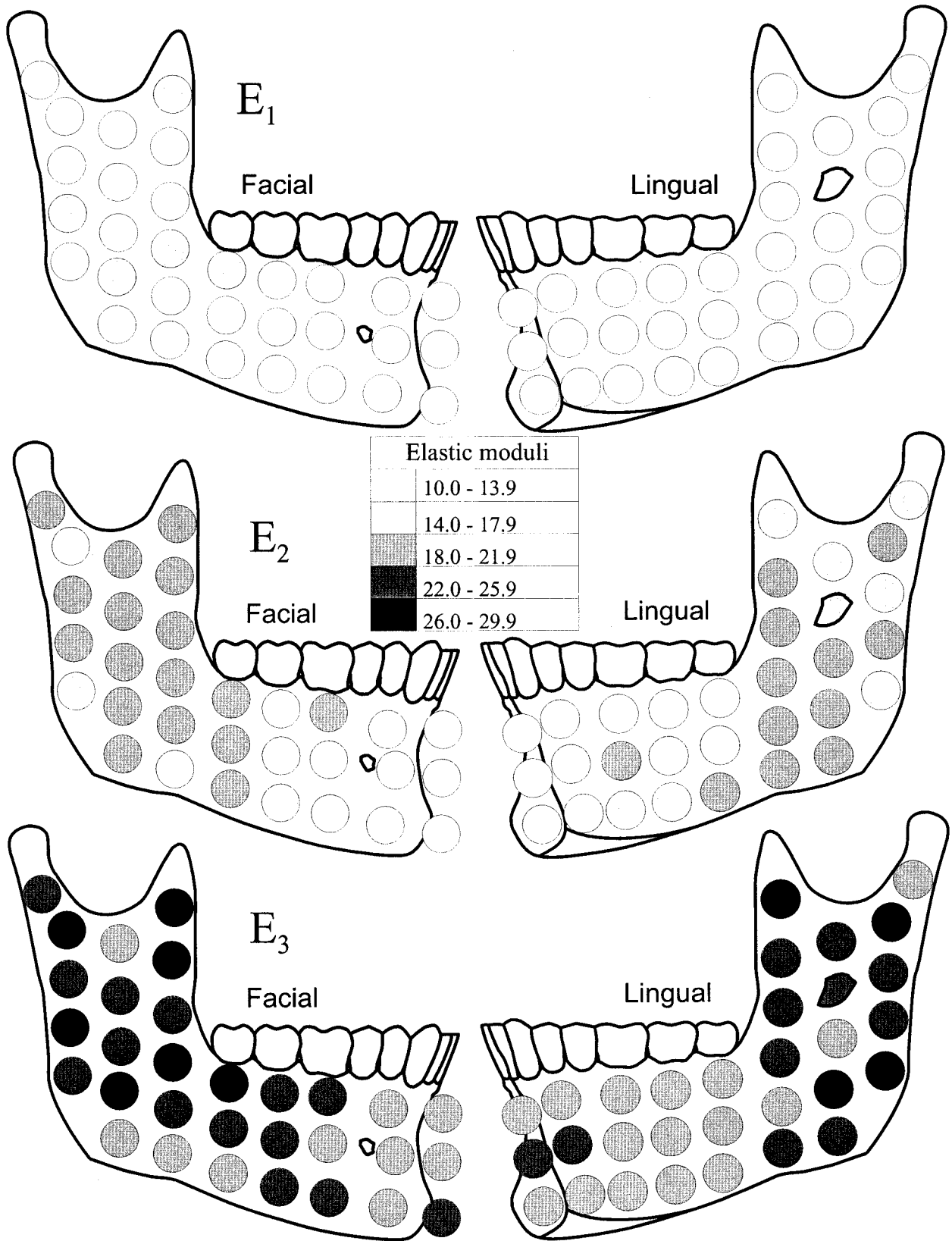


Fig. 5. Elastic moduli (GPa) for human dentate mandibles. **Top:** E_1 . **Middle:** E_2 . **Bottom:** E_3 . Larger values indicate stiffer bone in the specified direction.

TABLE 4. Elastic and shear moduli (in GPa) for human dentate mandibles¹

St	Sd	Area	E ₁		E ₂		E ₃		G ₁₂		G ₃₁		G ₂₃	
			Mean	SD	Mean	SD	Mean	SD	Mean	SD	Mean	SD	Mean	SD
1	F	Sym	12.1	2.0	14.8	1.3	22.0	4.2	4.4	0.9	4.7	0.5	6.3	0.8
2	F	Sym	11.8	1.4	15.9	1.9	21.4	4.2	4.7	0.6	5.2	0.7	7.2	0.7
3	F	Infbor	12.3	1.7	16.6	2.3	23.0	3.1	4.9	0.9	5.5	0.8	7.7	0.8
4	F	Infbor	13.0	1.8	17.9	1.7	25.0	4.3	5.0	0.5	5.6	0.7	7.8	0.9
5	F	Infbor	12.1	1.2	18.4	2.3	21.8	3.8	4.9	0.3	5.6	0.6	7.6	0.8
6	F	Angle	11.2	0.9	17.3	1.5	19.1	3.3	4.8	0.4	5.2	0.4	7.6	0.3
7	F	Angle	11.5	1.1	18.8	2.9	21.1	5.5	4.6	0.4	5.0	0.2	6.9	0.7
8	F	Sym	11.0	1.2	15.8	2.8	19.5	4.6	4.3	0.5	4.8	0.6	6.4	0.8
9	F	Sym	11.5	1.2	14.6	1.5	19.8	4.0	4.6	0.4	5.2	0.6	7.2	0.9
10	F	Midbod	11.9	2.2	18.0	2.9	20.3	5.7	4.8	0.5	5.4	0.9	7.4	1.3
11	F	Midbod	13.0	1.3	17.6	3.0	22.5	5.6	5.1	0.5	5.8	0.5	7.6	0.6
12	F	Midbod	13.7	1.4	19.2	1.3	24.2	4.5	5.3	0.7	5.8	0.7	7.9	0.5
13	F	Midram	13.6	1.6	19.3	1.5	25.5	4.5	5.0	0.3	5.9	0.5	7.8	0.6
14	F	Angle	14.0	1.7	19.8	2.3	28.5	5.5	5.2	0.8	5.8	0.7	7.9	0.3
15	F	Posbor	13.2	1.0	17.0	1.6	25.1	3.1	4.8	0.5	5.5	0.7	7.4	0.7
16	F	Sym	11.2	1.1	14.8	2.6	18.3	4.3	4.5	0.7	4.7	0.6	5.7	0.7
17	F	Sym	11.5	1.6	16.4	2.1	19.0	4.5	4.9	0.9	5.3	0.8	6.6	0.7
18	F	Alv	13.0	1.9	18.7	1.8	22.2	4.1	5.2	0.6	5.4	0.5	7.5	0.7
19	F	Alv	13.8	2.8	17.6	2.7	23.8	6.8	5.3	0.7	5.8	0.7	7.6	0.6
20	F	Alv	14.1	2.1	18.4	2.1	26.2	6.9	5.4	0.7	5.9	0.8	7.9	1.0
21	F	Midram	14.3	1.8	20.5	2.4	27.8	4.8	5.1	0.6	5.8	0.5	8.2	0.6
22	F	Midram	12.9	1.9	18.6	1.6	23.5	4.7	5.3	0.8	5.7	0.9	7.8	0.8
23	F	Posbor	14.0	2.0	18.8	1.8	27.3	6.5	5.4	0.7	5.6	0.4	7.8	0.7
24	F	Midram	12.9	1.0	19.3	1.4	22.7	4.6	4.9	0.6	5.4	0.7	7.7	0.5
25	F	Midram	12.9	1.7	19.9	1.1	23.8	5.1	5.2	0.5	5.6	0.5	7.6	0.7
26	F	Posbor	13.7	1.9	18.6	1.7	25.9	7.2	5.2	0.4	5.5	0.5	7.6	0.7
27	F	Cor	13.9	1.8	20.2	2.2	27.3	5.2	5.2	0.6	5.7	0.4	7.8	0.7
28	F	Midram	11.5	1.8	19.3	2.6	19.6	3.4	5.0	0.5	5.5	0.7	7.7	0.7
29	F	Cond	13.3	1.7	17.7	1.3	26.6	5.5	4.9	0.6	5.5	0.3	7.7	0.5
30	F	Cor	14.1	2.1	18.9	1.8	29.8	6.4	5.2	0.4	5.8	0.7	7.5	0.7
31	F	Cond	13.1	1.7	18.3	1.5	25.3	4.1	5.2	0.6	5.6	0.7	7.2	0.4
1	L	Sym	12.2	2.3	16.6	2.1	18.5	4.7	5.2	0.6	5.9	0.8	7.1	1.0
2	L	Sym	13.0	2.3	16.9	1.4	21.1	5.5	5.2	0.7	6.0	0.7	7.6	0.8
3	L	Infbor	12.9	2.1	17.0	3.4	22.0	6.6	5.1	0.6	5.7	0.4	7.6	0.9
4	L	Infbor	12.3	2.0	17.7	2.3	21.0	3.2	5.0	0.7	5.5	0.8	7.5	0.8
5	L	Infbor	12.5	1.7	18.8	1.3	20.7	3.1	5.0	0.6	5.4	0.6	7.8	0.6
6	L	Angle	12.7	1.8	20.2	2.6	22.9	4.1	5.0	0.6	5.5	0.6	8.0	0.7
7	L	Angle	12.6	1.1	18.6	2.5	22.3	4.5	5.1	0.5	5.4	0.6	7.5	0.8
8	L	Sym	13.1	1.7	17.5	1.5	22.0	5.2	5.0	0.5	5.7	0.5	7.2	0.8
9	L	Sym	13.2	1.4	17.9	1.5	22.8	6.2	5.3	0.4	5.7	0.4	7.6	0.7
10	L	Midbod	12.1	1.3	19.2	2.2	20.1	3.7	4.9	0.3	5.5	0.5	7.6	0.8
11	L	Midbod	11.7	1.6	18.1	2.4	17.9	2.6	5.0	0.5	5.4	0.6	7.0	0.8
12	L	Midbod	11.6	1.9	18.0	3.2	19.0	3.7	5.1	0.7	5.0	0.6	7.1	0.8
13	L	Midram	12.4	1.3	19.6	1.6	20.0	2.5	5.1	0.6	5.1	0.7	7.4	0.6
14	L	Angle	13.2	2.4	21.1	2.1	26.4	6.3	5.0	0.5	5.8	1.1	8.1	0.4
15	L	Posbor	12.1	1.3	17.3	2.6	26.7	5.3	4.5	0.5	5.2	0.5	6.7	0.6
16	L	Sym	12.1	1.5	17.7	1.8	19.5	3.7	4.9	0.6	5.1	0.6	6.5	0.4
17	L	Sym	12.4	1.6	17.3	2.5	22.0	6.0	4.9	0.6	5.5	0.7	7.5	0.6
18	L	Alv	13.4	1.2	16.3	2.0	21.4	3.0	5.2	0.7	5.5	0.4	6.9	0.5
19	L	Alv	12.6	1.9	16.2	2.6	20.2	5.0	5.2	0.6	5.3	0.5	6.8	0.6
20	L	Alv	12.6	2.1	17.2	1.9	19.8	4.3	5.1	0.7	5.5	0.6	6.8	0.6
21	L	Midram	12.5	1.6	19.0	2.2	22.4	3.0	5.0	0.6	5.6	0.6	7.5	0.7
22	L	Midram	12.4	1.9	19.1	3.4	21.8	5.5	5.3	1.0	5.4	0.7	7.3	0.8
23	L	Posbor	12.9	1.8	18.2	2.3	25.9	4.7	4.9	0.5	5.2	0.6	6.9	0.7
24	L	Midram	12.8	2.0	18.2	2.8	24.1	5.5	5.0	0.8	5.3	0.6	7.3	0.7
25	L	Midram	12.1	2.1	17.7	2.5	23.7	6.7	4.8	0.4	5.2	0.6	6.9	1.0
26	L	Posbor	12.5	1.4	16.5	2.9	23.2	4.3	4.7	0.7	5.0	1.0	6.8	0.8
27	L	Cor	12.6	1.5	18.4	1.7	24.8	5.2	5.0	0.2	5.1	0.7	7.4	0.5
28	L	Midram	13.4	1.4	16.1	2.4	23.1	3.0	5.0	0.4	5.5	0.7	7.0	1.1
29	L	Cond	13.1	1.1	18.1	1.9	26.5	4.1	5.0	0.5	5.3	0.5	7.5	0.7
30	L	Cor	13.9	2.7	16.1	0.8	26.2	9.4	5.4	0.6	5.7	1.0	6.8	1.3
31	L	Cond	12.2	1.5	17.4	2.0	21.7	4.9	5.1	0.8	5.4	0.7	7.1	0.5

¹ See Table 2 for abbreviations.

for the applied load and response directions are not equal, the magnitudes of the ratios differ. On the facial cortex, larger ν_{21} ratios were found at the condylar neck, coronoid process, angle, and inferior

symphyseal sites. This facial pattern was less distinct for ν_{12} . On the lingual cortex, regions with larger values of ν_{12} included the coronoid process, beneath the premolars and first molar, mid-symphy-

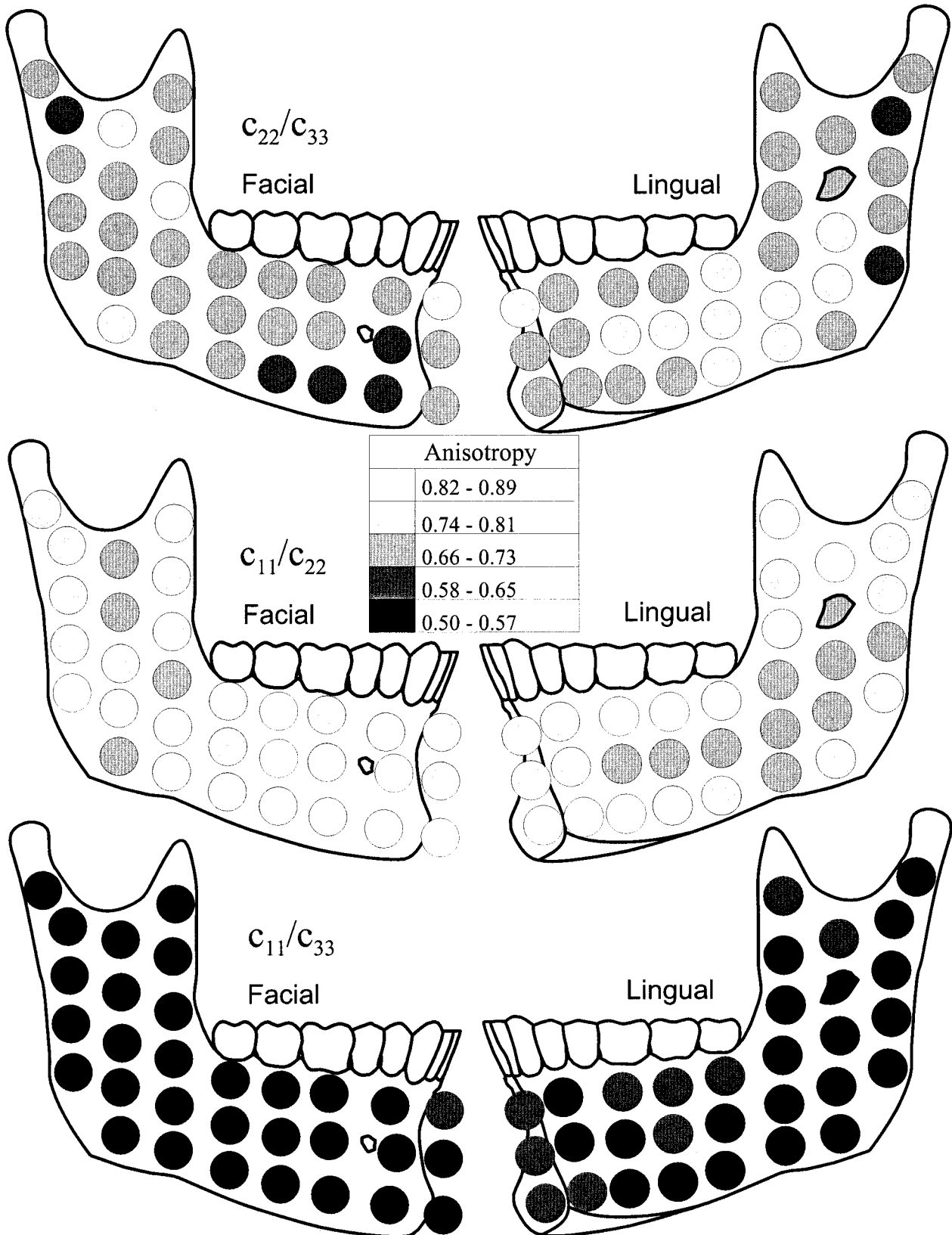


Fig. 6. Anisotropy for human dentate mandibles. **Top:** c_{22}/c_{33} . **Middle:** c_{11}/c_{22} . **Bottom:** c_{11}/c_{33} . Smaller ratios indicate larger anisotropy.

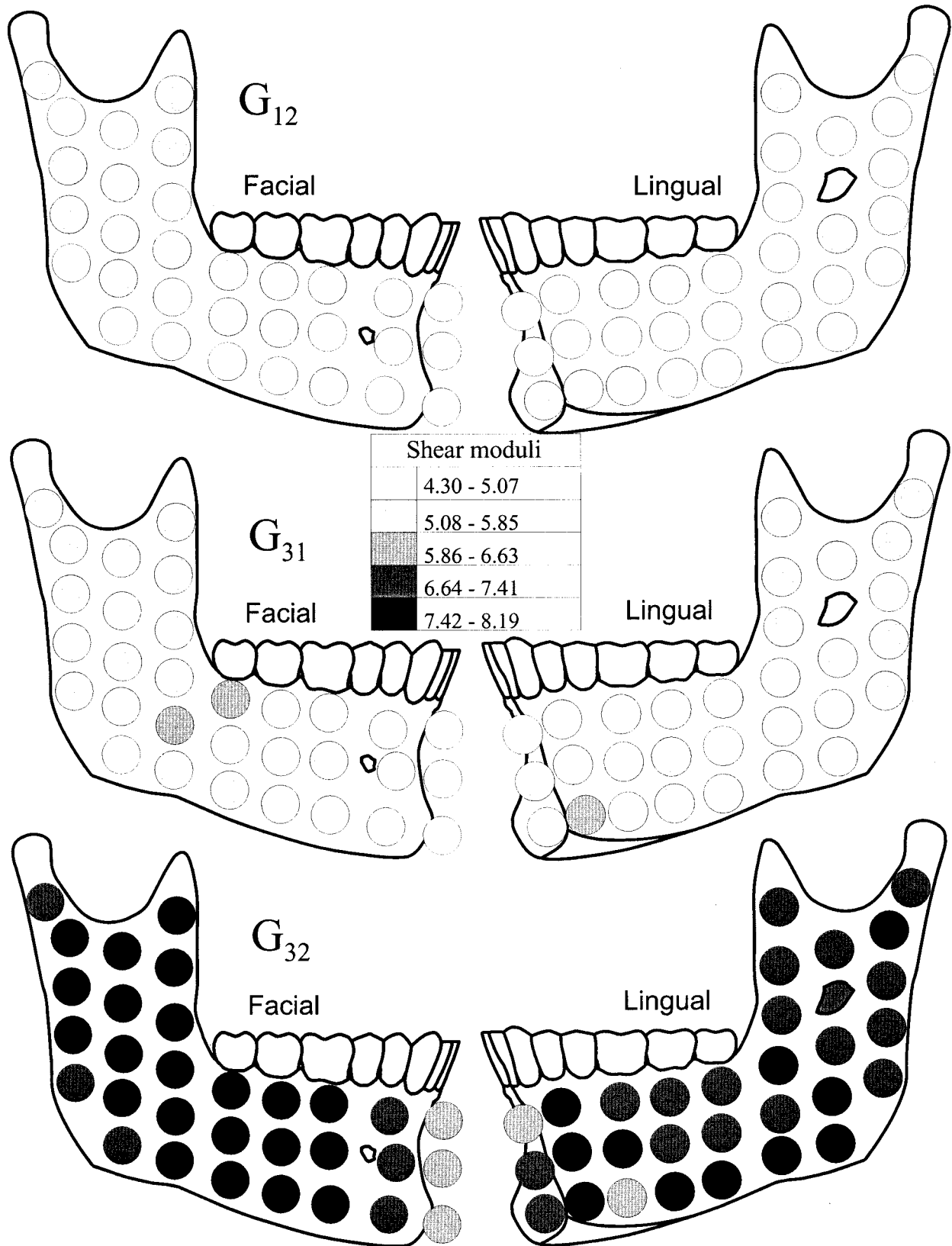


Fig. 7. Shear moduli (GPa) for human dentate mandibles. **Top:** G_{12} . **Middle:** G_{31} . **Bottom:** G_{32} . Larger values indicate stiffer bone in the specified plane.

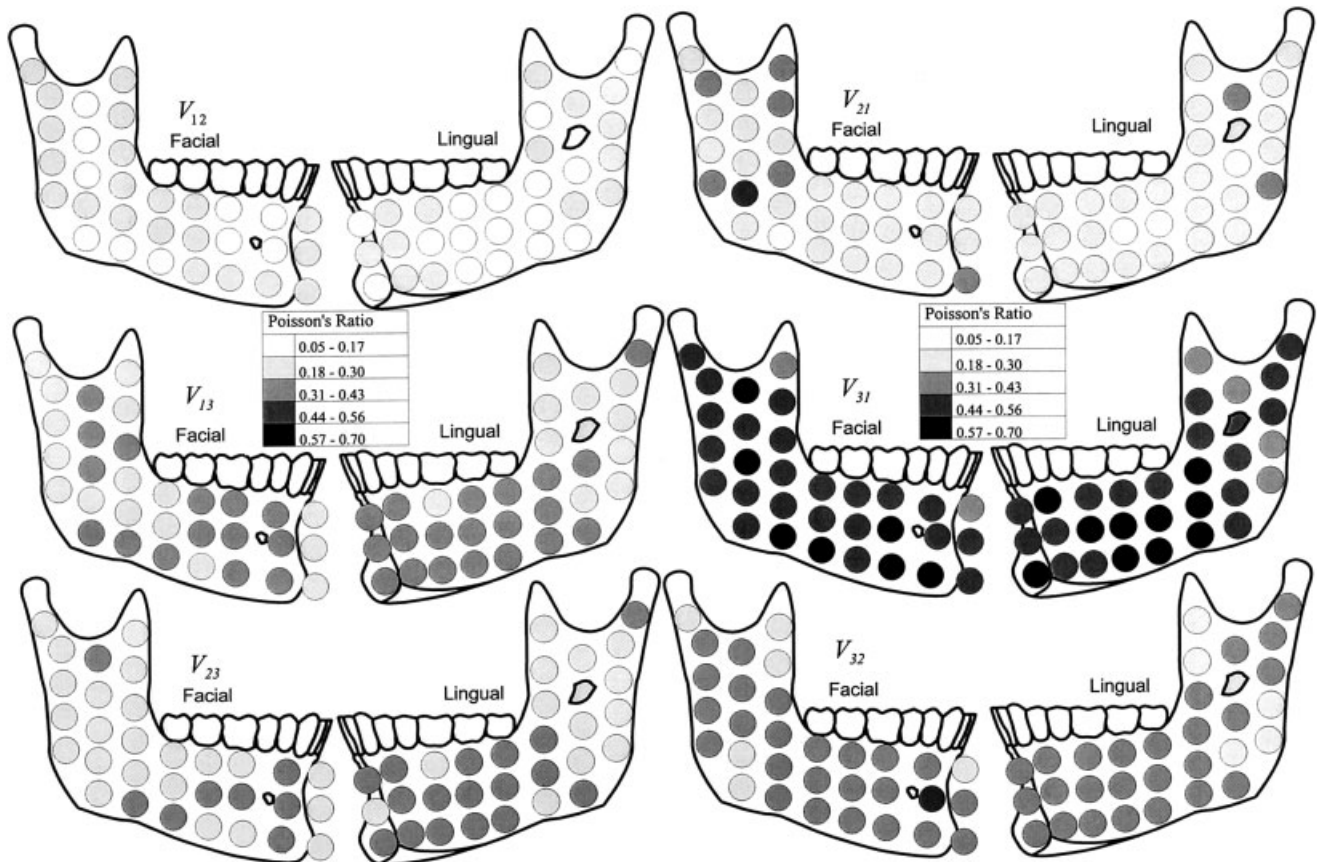


Fig. 8. Poisson's ratios for human dentate mandibles. **Top:** ν_{12} and ν_{21} . **Middle:** ν_{13} and ν_{31} . **Bottom:** ν_{23} and ν_{32} . Larger values indicate larger deformation in the direction indicated by the second subscript when force is applied in the direction of the first subscript.

sis, the posterior border of the ramus, and the sigmoid notch. This lingual pattern was less distinct for ν_{21} .

Patterns for ν_{13} and ν_{31} values were similar. Facially, larger ratios were located at the inferior border of the corpus and mid-ramus sites, while smaller ratios were found at the symphysis and coronoid process. Lingually, there were larger ratios throughout most of the corpus, and smaller ratios at the posterior border of the ramus, the sigmoid notch, and the coronoid process.

Patterns for ν_{23} and ν_{32} were similar lingually but less so facially. Lingually, smaller ratios were located in the ramus and coronoid process. Facially, smaller ratios were found at the symphysis, condylar process, coronoid process, and angle, although ν_{23} had a larger range throughout the ramus and posterior corpus.

Correlations between variables

With two exceptions, cortical thickness, cortical density, anisotropy, elastic and shear moduli, and Poisson's ratio did not differ by gender and showed no significant correlations of mean values with age. The exceptions were significant negative correlations ($R = -0.85$ and $R = -0.81$) between both G_{12} and G_{31} and age (Fig. 9).

Effects of material property variation on stresses calculated from bone strains

Effects of variation in material anisotropy and orientation on the calculation of stress orientations and magnitudes from strain when $\epsilon_q/\epsilon_p = 1.0$. $\Delta\Phi$ peaked when $\Delta\alpha$ was 30° or 60° for all values of E_2/E_3 (Fig. 10A). The largest $\Delta\Phi$ ($\pm 12.9^\circ$) was found at $E_2/E_3 = 0.9$ (Fig. 10A). σ_q/σ_p error increased as anisotropy and $\Delta\alpha$ increased. At the maximum, σ_q/σ_p was underestimated by about 75% when $E_2/E_3 = 0.5$ and $\Delta\alpha = 90^\circ$ (Fig. 10B). For all anisotropies, if $\Delta\alpha$ was 45° , then σ_q/σ_p was 1.0, which incorrectly suggested material isotropy.

Effects of variation in material orientation on the calculation of stress orientations and magnitudes from strain when ϵ_q/ϵ_p ranged from 0.5–3.0. For $\Delta\alpha = 25^\circ, 45^\circ, \text{ or } 65^\circ$, ϵ_q/ϵ_p increased exponentially relative to $\Delta\Phi$ (Fig. 11A). If $\Delta\alpha = 0^\circ$ or 90° , then $\Delta\Phi = 0$. If $\Delta\alpha = 25^\circ$ and $\epsilon_q/\epsilon_p = 3.0$, then $\Delta\Phi = 13.2^\circ$, which was similar to the maximum $\Delta\Phi$ of 12.9° from Figure 10A. If $\Delta\alpha = 65^\circ$ and $\epsilon_q/\epsilon_p = 0.5$, then $\Delta\Phi = -12.3^\circ$, which was nearly identical to the minimum $\Delta\Phi$ of -12.9° from Figure 10A. If measured strains indicate that $\epsilon_q/\epsilon_p = 1.0$ and $\Delta\alpha = 45^\circ$, then $\Delta\Phi = 0^\circ$, which might suggest incorrectly that 1) $\Delta\alpha = 0^\circ$, meaning the material

TABLE 5. Poisson's ratios for human dentate mandibles¹

St	Sd	Area	ν_{12}		ν_{13}		ν_{21}		ν_{23}		ν_{31}		ν_{32}	
			Mean	SD	Mean	SD	Mean	SD	Mean	SD	Mean	SD	Mean	SD
1	F	Sym	0.28	0.10	0.25	0.09	0.34	0.10	0.23	0.08	0.44	0.13	0.32	0.08
2	F	Sym	0.18	0.09	0.34	0.07	0.23	0.12	0.32	0.08	0.60	0.07	0.41	0.06
3	F	Infbor	0.20	0.13	0.31	0.05	0.26	0.16	0.29	0.06	0.58	0.08	0.40	0.05
4	F	Infbor	0.19	0.11	0.29	0.06	0.26	0.14	0.27	0.06	0.56	0.10	0.37	0.05
5	F	Infbor	0.14	0.09	0.34	0.09	0.21	0.13	0.31	0.09	0.59	0.08	0.36	0.06
6	F	Angle	0.10	0.06	0.40	0.07	0.15	0.09	0.38	0.07	0.66	0.05	0.41	0.04
7	F	Angle	0.14	0.07	0.31	0.11	0.22	0.11	0.28	0.10	0.54	0.11	0.30	0.07
8	F	Sym	0.18	0.09	0.30	0.11	0.25	0.12	0.28	0.11	0.50	0.12	0.33	0.10
9	F	Sym	0.17	0.09	0.33	0.13	0.21	0.10	0.35	0.09	0.54	0.17	0.46	0.10
10	F	Midbod	0.15	0.09	0.37	0.10	0.22	0.12	0.34	0.10	0.61	0.10	0.36	0.06
11	F	Midbod	0.19	0.09	0.34	0.11	0.25	0.10	0.32	0.11	0.55	0.11	0.38	0.08
12	F	Midbod	0.20	0.09	0.30	0.09	0.27	0.12	0.27	0.09	0.51	0.10	0.33	0.06
13	F	Midram	0.22	0.11	0.28	0.08	0.30	0.14	0.25	0.08	0.52	0.10	0.32	0.06
14	F	Angle	0.23	0.11	0.23	0.09	0.31	0.13	0.21	0.09	0.45	0.14	0.28	0.08
15	F	Posbor	0.26	0.10	0.25	0.07	0.33	0.11	0.23	0.07	0.47	0.13	0.32	0.07
16	F	Sym	0.21	0.12	0.27	0.09	0.26	0.13	0.25	0.09	0.42	0.12	0.29	0.06
17	F	Sym	0.15	0.16	0.35	0.11	0.19	0.16	0.33	0.11	0.56	0.14	0.36	0.06
18	F	Alv	0.17	0.11	0.33	0.07	0.23	0.13	0.30	0.07	0.55	0.11	0.35	0.05
19	F	Alv	0.22	0.14	0.31	0.12	0.27	0.16	0.29	0.12	0.50	0.14	0.36	0.09
20	F	Alv	0.22	0.12	0.28	0.11	0.29	0.16	0.26	0.12	0.49	0.12	0.34	0.10
21	F	Midram	0.23	0.11	0.23	0.09	0.31	0.13	0.25	0.11	0.45	0.17	0.33	0.12
22	F	Midram	0.14	0.09	0.33	0.07	0.20	0.12	0.30	0.07	0.59	0.09	0.37	0.06
23	F	Posbor	0.21	0.12	0.26	0.09	0.27	0.15	0.24	0.09	0.49	0.11	0.32	0.07
24	F	Midram	0.19	0.11	0.32	0.10	0.28	0.16	0.28	0.12	0.53	0.09	0.31	0.08
25	F	Midram	0.15	0.10	0.31	0.09	0.22	0.13	0.29	0.10	0.56	0.13	0.33	0.07
26	F	Posbor	0.22	0.13	0.27	0.12	0.29	0.15	0.25	0.12	0.48	0.17	0.31	0.10
27	F	Cor	0.22	0.09	0.25	0.07	0.31	0.11	0.22	0.07	0.47	0.10	0.28	0.05
28	F	Midram	0.12	0.09	0.39	0.06	0.20	0.13	0.32	0.13	0.66	0.15	0.33	0.13
29	F	Cond	0.24	0.11	0.25	0.10	0.32	0.13	0.23	0.10	0.48	0.15	0.32	0.08
30	F	Cor	0.25	0.14	0.19	0.09	0.31	0.16	0.18	0.08	0.39	0.14	0.26	0.09
31	F	Cond	0.20	0.07	0.26	0.09	0.27	0.09	0.22	0.07	0.49	0.16	0.29	0.08
1	L	Sym	0.15	0.11	0.40	0.10	0.20	0.12	0.36	0.11	0.60	0.14	0.38	0.09
2	L	Sym	0.19	0.12	0.35	0.11	0.24	0.14	0.33	0.11	0.54	0.14	0.38	0.07
3	L	Infbor	0.18	0.12	0.34	0.13	0.23	0.16	0.32	0.13	0.54	0.13	0.39	0.12
4	L	Infbor	0.15	0.08	0.35	0.08	0.21	0.09	0.33	0.08	0.59	0.11	0.38	0.08
5	L	Infbor	0.15	0.06	0.37	0.06	0.23	0.08	0.34	0.06	0.60	0.08	0.37	0.05
6	L	Angle	0.17	0.13	0.32	0.09	0.25	0.16	0.29	0.10	0.57	0.10	0.32	0.05
7	L	Angle	0.16	0.08	0.33	0.07	0.23	0.10	0.31	0.07	0.56	0.07	0.36	0.05
8	L	Sym	0.22	0.12	0.32	0.10	0.28	0.13	0.30	0.10	0.52	0.10	0.35	0.05
9	L	Sym	0.18	0.11	0.33	0.11	0.23	0.14	0.31	0.11	0.54	0.12	0.37	0.08
10	L	Midbod	0.14	0.10	0.37	0.09	0.21	0.12	0.34	0.09	0.60	0.10	0.34	0.05
11	L	Midbod	0.10	0.07	0.39	0.06	0.15	0.10	0.37	0.06	0.60	0.07	0.36	0.04
12	L	Midbod	0.09	0.06	0.38	0.06	0.14	0.09	0.36	0.06	0.61	0.08	0.38	0.06
13	L	Midram	0.13	0.09	0.36	0.06	0.19	0.12	0.33	0.07	0.57	0.09	0.33	0.05
14	L	Angle	0.18	0.08	0.25	0.14	0.28	0.10	0.23	0.15	0.49	0.22	0.26	0.13
15	L	Posbor	0.23	0.15	0.20	0.09	0.31	0.18	0.18	0.09	0.43	0.14	0.27	0.09
16	L	Sym	0.16	0.07	0.34	0.09	0.23	0.09	0.31	0.09	0.53	0.09	0.33	0.05
17	L	Sym	0.18	0.10	0.34	0.10	0.25	0.12	0.31	0.10	0.57	0.11	0.37	0.07
18	L	Alv	0.25	0.13	0.30	0.07	0.29	0.12	0.28	0.07	0.47	0.10	0.36	0.05
19	L	Alv	0.17	0.10	0.34	0.11	0.21	0.11	0.32	0.11	0.51	0.11	0.38	0.09
20	L	Alv	0.17	0.08	0.35	0.09	0.23	0.10	0.32	0.10	0.53	0.09	0.36	0.05
21	L	Midram	0.15	0.10	0.32	0.08	0.22	0.12	0.31	0.08	0.57	0.09	0.35	0.04
22	L	Midram	0.12	0.07	0.32	0.09	0.17	0.09	0.30	0.09	0.55	0.11	0.33	0.07
23	L	Posbor	0.21	0.10	0.19	0.12	0.28	0.10	0.21	0.12	0.37	0.22	0.27	0.13
24	L	Midram	0.19	0.13	0.27	0.11	0.26	0.15	0.26	0.11	0.49	0.12	0.32	0.07
25	L	Midram	0.16	0.11	0.26	0.13	0.23	0.14	0.25	0.12	0.47	0.17	0.30	0.10
26	L	Posbor	0.24	0.08	0.25	0.07	0.30	0.07	0.23	0.07	0.46	0.10	0.32	0.06
27	L	Cor	0.17	0.10	0.26	0.09	0.24	0.13	0.24	0.09	0.49	0.14	0.30	0.10
28	L	Midram	0.27	0.09	0.25	0.11	0.32	0.07	0.23	0.10	0.42	0.17	0.32	0.11
29	L	Cond	0.22	0.10	0.25	0.09	0.30	0.11	0.23	0.09	0.49	0.14	0.31	0.09
30	L	Cor	0.26	0.20	0.20	0.15	0.28	0.20	0.20	0.14	0.34	0.20	0.26	0.12
31	L	Cond	0.14	0.08	0.32	0.11	0.19	0.10	0.31	0.10	0.54	0.14	0.36	0.08

¹ See Table 2 for abbreviations.

axis and strain axis are aligned; or 2) $\Delta\text{pa} = 90^\circ$, meaning the material and strain axis are perpendicular.

ϵ_q/ϵ_p was an increasingly poor predictor of σ_q/σ_p as anisotropy and ϵ_q/ϵ_p increased (Fig. 11B). The largest absolute errors were found when $\Delta\text{pa} = 0^\circ$. For

instance, when $E_2/E_3 = 0.6$ and $\Delta\text{pa} = 0^\circ$, σ_q/σ_p was more than 4 times larger than ϵ_q/ϵ_p .

Maximum calculation errors in the human mandible by site when $\epsilon_q/\epsilon_p = 1.0$. Sites were categorized into 4 groups according to the maximum

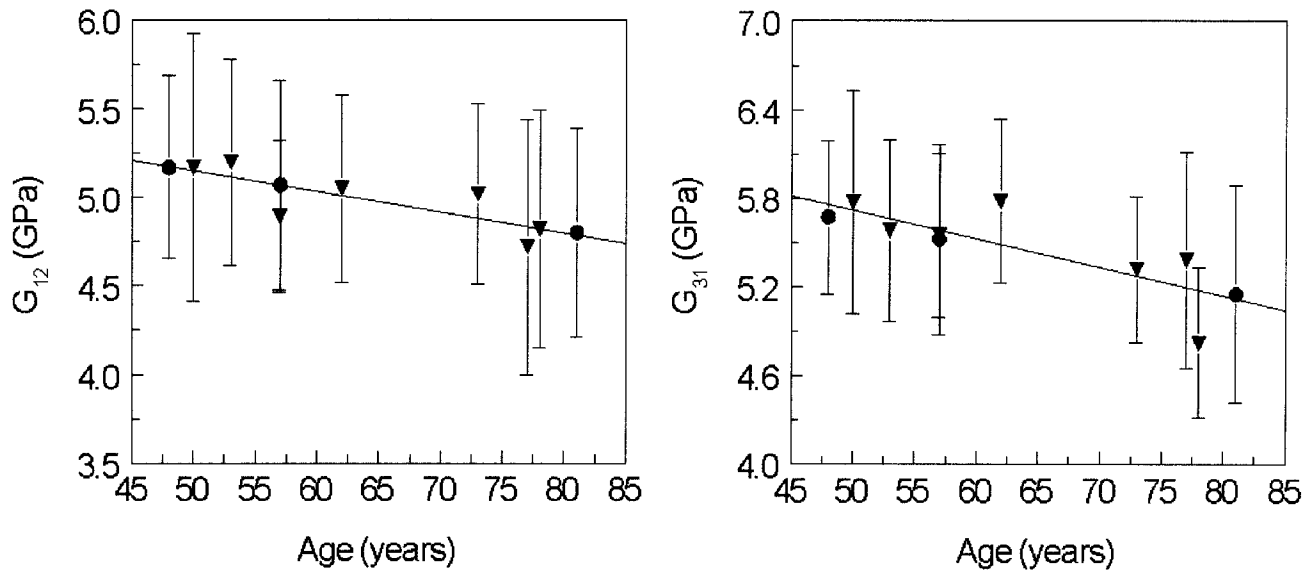


Fig. 9. Negative correlations between G_{12} and G_{31} with age. Male, ∇ ; female, \bullet . Error bars represent standard errors at the means.

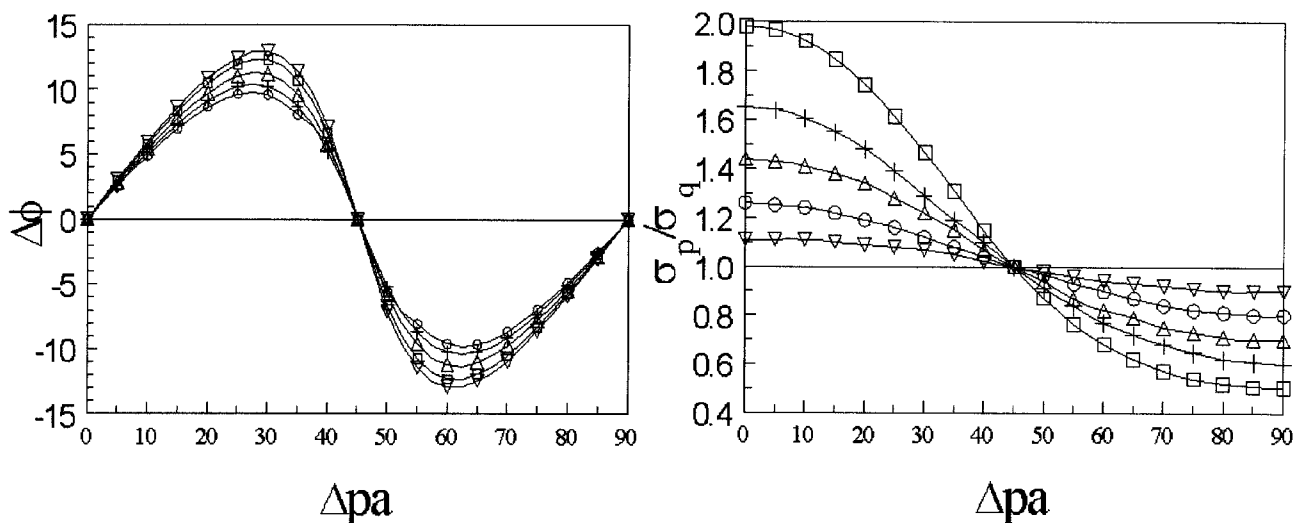


Fig. 10. Difference between principal strain orientation and material property orientation (Δpa) vs. $\Delta\Phi$ and σ_q/σ_p when $\epsilon_q/\epsilon_p = 1.0$. ϵ_p and ϵ_q are maximum and minimum principal strains; σ_p and σ_q are maximum and minimum principal stresses; $\Delta\Phi$ is the difference between angles of maximum principal strain and stress. All strains are in microstrain ($\mu\epsilon$), and all stresses are in MPa. All angles are in degrees. Symbols used to indicate amount of E_2/E_3 anisotropy: \square , 0.5; $+$, 0.6; \triangle , 0.7; \circ , 0.8; ∇ , 0.9.

errors in σ_q/σ_p ($\leq 10\%$, $>10\%$ and $\leq 20\%$, $>20\%$ and $\leq 30\%$, and $>30\%$), which occurred when stresses in individual mandibles were calculated using mean material properties for each site (Fig. 12). The majority of sites (37/62) had errors $\leq 10\%$. The sites with the largest errors ($>30\%$) were found in the facial cortex at the angular process, and at the alveolar and midportion of the symphysis. Errors $>20\%$ were also found at the coronoid process, near the mandibular notch, and inferior to the distal molar facially.

DISCUSSION

Orientation of material axes

This study is the first to explore variations in the direction of maximum stiffness throughout the cor-

tex of a bone. The human mandible is a good model for such a study because of its regional variations in function, and there is a significant available amount of cortical bone. Results show that variability in the direction of maximum stiffness ranged from sites with no statistically significant mean direction to those with little variation in mean direction. These variations suggest the importance of measuring material orientation in cortical bone prior to determining material properties by ultrasonic or mechanical methods.

Mean directions of maximum stiffness varied considerably among sites (Fig. 3, Table 2), as well as within sites. No common orientation can be assumed for mandibular cortical bone based on anatomical

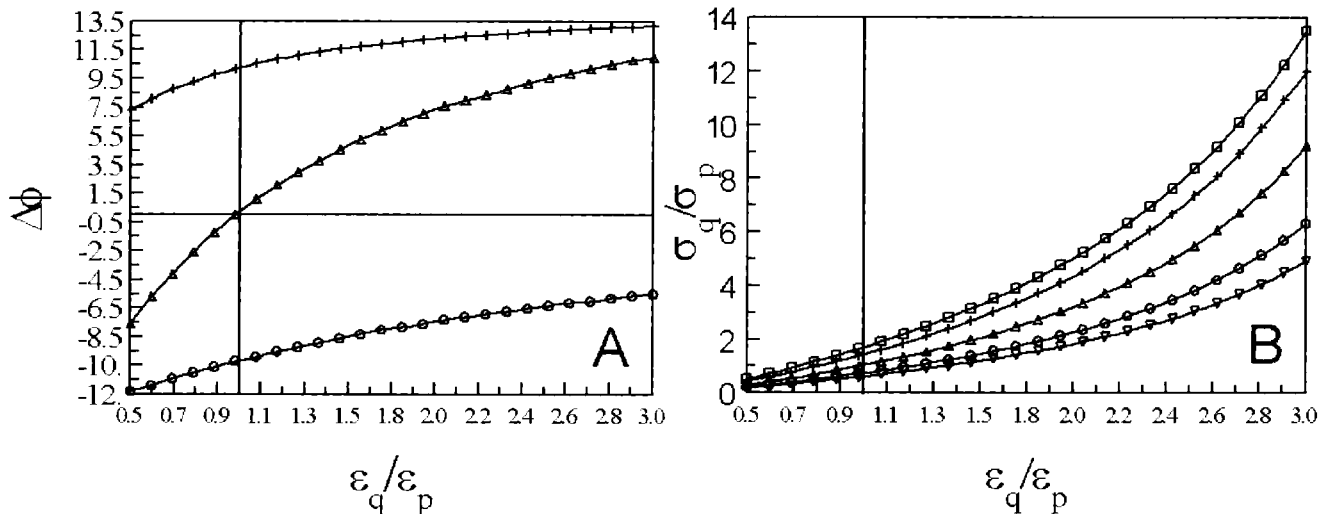


Fig. 11. Ratio of mean compressive and tensile strains (ϵ_q/ϵ_p) vs. (A) $\Delta\Phi$ and (B) σ_q/σ_p , when E_2/E_3 anisotropy = 0.6. ϵ_p and ϵ_q are maximum and minimum principal strains; σ_p and σ_q are maximum and minimum principal stresses; $\Delta\Phi$ is the difference between angles of maximum principal strain and stress. All angles are in degrees. \square , 0°; +, 25°; Δ , 45°; \circ , 65°; ∇ , 90°. Vertical line was set at $\epsilon_q/\epsilon_p = 1.0$, as discussed in the text.

features. Mandibular material orientations and cortical elastic moduli from previous studies fall within the range of variation from comparable sites in our study. Previous studies include 1) ultrasonic investigations by Carter (1989) on 37 coin-shaped specimens taken from 12 sites in 4 mandibles, and 2) mechanical tests on 5 sites from the facial corpus and ramus, using three-point bending (Tamatsu et al., 1996; Hara et al., 1998).

Mandibular trabecular orientations are similar to patterns of the direction of maximum stiffness found in the overlying cortical bone. Herzberg and Dovitch (1968), using 8 human mandibles ranging in age from 6 weeks prenatal through adult, radiographically study trabecular orientation in the mandibular ramus. They note that after the eruption of secondary teeth, trabeculations form a pattern oriented 1) between the mandibular angle and condyle and 2) between both the condyle and coronoid process and the retromolar area. This pattern is similar to the direction of maximum stiffness for the overlying cortical bone. Stereological studies of trabecular morphology of pig mandibular condyles (Teng and Herring, 1995, 1996) show dense and robust condylar trabeculae aligned in the supero-inferior direction. Micro-CT scans of embalmed adult human mandibular condyles and condylar necks (Giesen and van Eijden, 2000) find an inhomogeneous and anisotropic trabecular organization in which orientations are similar to those of pigs, and are on average 3.4 times stiffer in the direction of predominant trabecular orientation (Giesen et al., 2001). In the human condylar neck, trabeculae on average align at 73° to the horizontal axis. In the overlying cortical bone, we find that the facial direction of maximum stiffness is oriented at 63°. This similarity is less for the lingual axis of maximal stiffness, which is oriented at 50°.

As our methodology actually determines the direction of maximum stiffness in compact bone, it is relevant to compare our results with those of other studies that attempt to determine tissue orientation based on anatomical data. The only anatomical technique that is suggested to explicate material orientation in mandibular cortical bone is the study of split-lines of the periosteal surface. Split-lines are used historically to determine orientation or "grain" of bone (Benninghoff, 1925). They demonstrate the histological organization of compact bone (Tappen, 1954, 1970; Buckland-Wright, 1977), including orientation of Haversian systems (Seipel, 1948; Tappen, 1967), although the precision of this determination is unclear. Buckland-Wright (1977), following comparisons of split-lines with ultrastructural features in 5 adult female cat skulls, concludes that split-lines form along regions of weakness such as cement-lines, interlamellar interfaces, lacunae, and vascular canals.

Such ultrastructural features are likely important in the orientation of bone tissue. It is suggested that the direction of maximum stiffness in cortical bone results from the orientation of osteons, lamellae, collagen fibers, apatite crystals, or other features of the matrix (Bouvier and Hylander, 1996; Dechow et al., 1993; Fratzl et al., 1992; Hara et al., 1998; Lipson and Katz, 1984; Petrtyl et al., 1996; Turner et al., 1995; Weiner et al., 1999). However, these possibilities have not been adequately tested, although they are based on qualitative observational data. For example, based on histologic cross sections, it is commonly accepted that osteons are primarily oriented longitudinally in the diaphysis of long bones. Correlated with this observation are the results of mechanical and ultrasonic tests, which show that the elastic modulus is greatest in that direction compared to circumferential or tangential orientations,

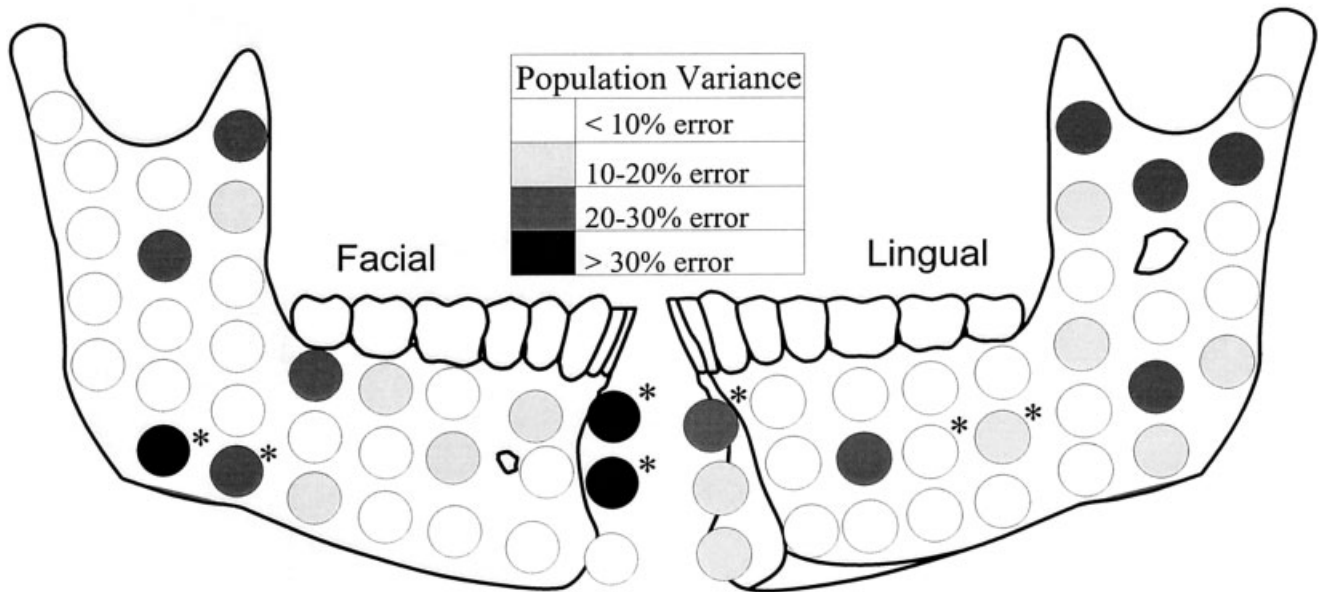


Fig. 12. Distribution of maximum potential calculation errors in human mandibles by site. *Nonoriented sites. Increasing errors of calculated σ_p/σ_p are seen at the facial alveolar process, lingual angle, and both cortices at the symphysis, and around the sigmoid notch.

and that anisotropy is prevalent in the mineral component of the bone matrix and less so in the organic component (Hasegawa et al., 1994; Turner et al., 1995; Takano et al., 1999).

If common ultrastructural features are determinants of both the results of split-line studies and the material orientation of bone tissue, do the orientations of mandibular split-lines resemble those found in this study? Split-line patterns for human mandibles (Seipel, 1948) greatly resemble our material orientations. Although the patterns are similar throughout the mandible, examples illustrate the detail of the similarities, such as in the alveolar process inferior to the canine- P_3 and in the coronoid process, where split-lines parallel the more vertical orientation of the direction of maximal stiffness.

Further, we expect that greater variation in split-line patterns are found in mandibular regions with either 1) increased variation in stiffness orientation, or with 2) no significant mean direction. This is difficult to assess in human mandibles, as Seipel (1948) provides minimal information on variation in split-line patterns. Tappen (1970) documents such variation in 5 baboon mandibles and notes that increased variability is found among individuals within the sigmoid notch region, a location in which we also found larger variations in the orientations of human cortical bone stiffness. However, Tappen (1970) does not note larger split-line variations in the angular and symphyseal alveolar regions of baboons, which are highly variable and do not have significant mean orientations in human mandibles. The lack of orientation at these sites is influenced by low anisotropy, as by definition isotropic sites have no direction of maximum stiffness. The biomechanical and structural differences between human and

baboon mandibles make these direct comparisons tenuous, but variability of split-lines in the sigmoid notch region is noteworthy because of similarities in masticatory muscle attachment and presumably masticatory function between species in this region.

Several factors account for the discrediting of split-lines as a useful morphological tool. One problem is a lack of specificity as to what aspects of structure are actually shown by split-lines. However, some reliable information exists on this topic (see references above). The larger problem is the idea that structure in bone reflects patterns of bone loading during common activities. Just as trabecular orientation is hypothesized to reflect load orientation in cancellous bone, cortical material orientation, as illustrated by split-lines, is hypothesized to reflect primary directions of stress in the cortical component of a bone. At the least, split-line patterns are thought to represent a histological response of bone to the mechanical environment (Tappen, 1954, 1967, 1970). However, split-line patterns do not correspond with principal strains in bone (Bouvier and Hylander, 1981; Buckland-Wright, 1977), and thus they are of little use for deriving patterns of bone loading.

As our macaque studies suggest (Dechow and Hylander, 2000), it is also unlikely that the direction of maximum stiffness in mandibular cortical bone aligns with average directions of principal strain or stress. Theoretical speculations about how bone microstructure adapts to loading patterns, which would influence the orientation of the elastic properties, include studies on how osteon orientation is directed by patterns of bone loading (Martin et al., 1998; Smit and Burger, 2000). It is unclear how these theoretical influences work in a complex man-

dibular mechanical environment, in which multiple loading patterns during mastication and biting depend on bolus position. An integration of the patterns of principal stresses during all frequent loadings do not result in a pattern resembling a single loading regime, so even if material orientation in bone is controlled by function, it is not comparable to any single stress pattern.

A comparison of the direction of maximum stiffness and the orientation of split-lines is interesting because it emphasizes the structural basis of material orientation in bone and its distinction from the related topic of how function might relate to or cause material adaptation. This distinction is essential as we try to understand development and adaptation in patterns of bone matrix microstructure and the complexities of its relationship to function. Recent studies of the lack of congruence of strain patterns and optimal gross form in sheep skulls (Thomason et al., 2001) and macaque tibiae (Demes et al., 2001) reflect the hierarchical nature of this problem in bone biology.

Even if split-lines tell us something useful about material orientation, they provide no information on material properties or anisotropy. Overall, there is a significant correlation ($R = 0.39$, $P = 0.002$) between the standard deviation for the direction of maximal stiffness and the mean E_2/E_3 for all sites, indicating a weak trend for more oriented sites to be more anisotropic. A region of bone can have consistency in material orientation among individuals and yet have relatively low anisotropy. An example of this is found near the anterior insertion of masseter at the mandibular lower border (facial sites 5 and 6), where the standard deviation for the direction of maximal stiffness is less than 15° , but E_2/E_3 is greater than 0.9. Conversely, a cortical region can have larger variability in orientation and also have relatively greater anisotropy. An example of this is found on the coronoid process (facial and lingual site 30), where the standard deviation for the direction of maximal stiffness is near 30° and E_2/E_3 is approximately 0.7.

If bone material orientation is related at least in part to cumulative stresses, we might hypothesize that greater anisotropy relates to consistent loading at a site, or conversely, sites with near isotropy may have greater variation in stress patterns generated during common functions. Sites in the human mandible that most approach isotropy in the cortical plane are found in some muscle attachment areas of the ramus on both the lingual and facial sides (Table 2, Fig. 6). Variations in patterns of muscle function during oral activities could result in a variety of stress patterns in these regions. On the other hand, some muscle attachment areas have relatively large amounts of anisotropy, while portions of the lingual corpus have low anisotropy. The alveolar region of the symphysis also has low anisotropy, but this area also has low elastic moduli and no consistent direction of stiffness among individuals. To approach this

hypothesis, more information is needed on variations in loading patterns and stresses in the human mandible.

Likewise, if material orientation is related to mechanical stress, we might hypothesize that interindividual variation in the direction of maximum stiffness relates to individual differences in loading patterns and stress distributions, resulting from variations in muscle function and mandibular form. The impact of such variations on mandibular stress distributions has received little study.

Material properties

Variations are found both within and between mandibles for each of the material properties (Table 6). If sides are compared overall, the facial aspect is thicker and stiffer along the direction of maximum stiffness (E_3) than the lingual aspect. Regionally, the symphysis, corpus, and ramus differ from each other. Many symphyseal sites share a unique set of features: they are thicker at the inferior border, less dense, less anisotropic, and less stiff in both axial loading and shear than many sites in the corpus and ramus. Overall, sites in the ramus are thinner, denser, and stiffer than sites in the corpus and at the symphysis. Many sites in the corpus have intermediate values between those of the ramus and symphysis. Within the symphysis, corpus, and ramus, some material properties also differ between sites. The most notable differences are the lower thickness, density, and stiffness of the symphyseal alveolar sites compared to midbody and inferior border sites.

Our results demonstrate a greater degree of regional material property variation within human mandibular cortical bone than has been reported in other bones. This larger variation reflects the functional heterogeneity of the mandible and the limitations of postcranial studies, which focused on the diaphyses of long bones and included data from 20 sites on a bovine femur (van Buskirk et al., 1981), 20 sites on 3 human femora (Ashman et al., 1984), and 12 sites on 8 human tibiae (Rho, 1996).

The most extensive previous studies of the human mandible are the unpublished dissertation by Carter (1989), who reports individual elastic coefficients for 37 cylindrical and 39 brick specimens from various sites throughout 4 mandibles, and Dechow et al. (1992), who reports material properties for 77 brick specimens from the lower border of the corpus in 15 mandibles. Carter's results fall within the range of the current findings. In Dechow et al. (1992), the principal axes of the brick specimens are assumed from geometry, and thus ultrasonic velocities are measured "off-axis." The symphyseal sites and the lingual molar sites were measured "off-axis" by an average of 10° and had mean E_3 values within 6% of those in Table 4. The facial molar sites, which were measured "off-axis" by about 20° , had E_3 values that were 20% different.

TABLE 6. Summary of material property variation throughout human dentate mandibles

Region	Distinguishing features within each region
Symphysis	Cortex of alveolar process is least oriented. Cortex of inferior border is thickest. Facial cortex is less dense than lingual cortex.
Corpus	Cortex of facial inferior border is less stiff for G_{12} . Cortex of inferior border is most oriented portion. Facial cortex of alveolar process is oriented more vertically. Facial cortex is thicker than lingual cortex.
Ramus	Facial cortex is stiffer than lingual cortex for E_3 and G_{23} . Posterior border sites are oriented in direction of posterior border of mandible. Mid-ramus cortical sites have variable orientations. Facial cortex is thicker than lingual cortex. Facial cortex is stiffer than lingual cortex for E_3 and G_{23} . Cortex of angle was least stiff for shear moduli.
Region	Distinguishing features between regions
Symphysis	Symphysial cortical bone contains most nonoriented sites. Symphysial cortical bone is thicker than both other regions. Symphysial cortical bone is less dense than other regions facially. Symphysial cortical bone is less stiff for elastic moduli E_2 . Symphysial cortical bone is less stiff for all shear moduli facially.
Corpus	Symphysial cortical bone often has lowest value of Poisson's ratios. Cortical bone of corpus is thicker than that of ramus. Cortical bone of corpus has intermediate values of elastic moduli E_2 .
Ramus	Cortical bone of corpus is stiffer than that of symphysis for G_{23} . Cortical bone of ramus is thinnest of all regions. Cortical bone of ramus is stiffer than that of other regions for E_2 . Stiffest cortical bone (E_3) is found at sites in the ramus. Cortical bone of ramus is stiffer than that of symphysis for G_{23} .

Katz et al. (1984) and Reilly and Burstein (1974) suggest that remodeling transforms cortical bone from an orthotropic material to a more transversely isotropic material. Studies on adult postcranial bones (van Buskirk et al., 1981; Ashman et al., 1984; Rho, 1996) show E_1 and E_2 values that were more similar to each other than in the mandible. Average values of E_1 for all sites are 20–45% smaller than E_2 , indicating that mandibular cortical bone is best modeled as orthotropic rather than transversely isotropic. If the hypothesis of Katz et al. (1984) and Reilly and Burstein (1974) is valid, then this difference suggests that the adult femoral and tibial cortices are more heavily remodeled than mandibular cortices. A thickness effect may also be a factor, since cortical bone from diaphyses of human femora and tibiae tends to be thicker than the mandible. However, ultrasonic velocities in the direction of D_1 are not correlated with the thicknesses of the 600 specimens, indicating that differences in elastic moduli are not related overall to thickness of the mandibular cortex. Another possibility is that cortical bone in the mandible, compared to some postcranial diaphyses, has greater variation in the orientation of internal microstructural features, such as osteons, especially in the plane of the cortical plate, that result in stiffer bone in the direction of minimum stiffness in that plane.

Very little is known about the development of mandibular material properties during growth and aging. Although Ashman et al. (1985) found that immature canine mandibles appear to be elastically isotropic. Preliminary data from cortices of immature pig mandibles demonstrate orthotropy (Shindling and Dechow, 1996). Data from human mandibles

do not show significant correlations between any of the anisotropy ratios and age at death. However, the sample size is small and restricted to ages 48–81 years. Conversely, G_{12} and G_{31} do have significant negative correlations within this age range ($R = -0.85$, $R = -0.81$). These differences may reflect a subtle change in material organization with age.

Also, little is known about the maintenance of material properties or reorganization of the direction of maximum stiffness throughout life in any bone. Zioupos and Currey (1998) noted a 2.3% decrease in the elastic modulus per decade of later life, based on 3-point bending tests of femoral cortices from human males. Mean elastic moduli for all data from each mandible have negative correlations with age ($R = -0.43$ for E_1 , $R = -0.46$ for E_2 , $R = -0.23$ for E_3), but the small sample size of mandibles produces inadequate power for these moderate to weak correlations to be significant at $P = 0.05$.

Poisson's ratios, which relate primary and secondary deformation, show variation, in part resembling ratios between the elastic and shear moduli in different directions. The ratios have significant differences between the 3 perpendicular planes and regionally. We present all ratios, as this detail may be important in improving finite element models of mandible. In most studies, Poisson's ratio is averaged to a single value, although a few document all 6 ratios (Ashman et al., 1984; Dechow et al., 1992).

The cortical material property most reported in the literature is that of density, which exhibits low variance. Our results correspond with other studies (Ashman et al., 1984; Carter, 1989; Dechow et al., 1992, 1993; Henrikson and Wallenius, 1974), al-

though we demonstrate that density differs regionally within an individual, while most previous human studies were inconclusive on this point. Duterloo et al. (1974) show lower densities in the symphysis and alveolar process than midcorpus and along the inferior border in macaques. This pattern corresponds with human mandibles in the symphyseal region.

Several studies show changes in mandibular cortical density associated with age. Duterloo et al. (1974) document an increase in mean density with age until young adulthood, followed by a decrease in even older macaques. Henrikson and Wallenius (1974) demonstrate a decline in mean density with age for 50 edentulous human mandibles. This study may not be comparable, as our mandibles were dentate and presumably maintain higher occlusal loads throughout later life. We find no significant decline in density with age. However, our sample is small and lacked power. The correlation between age and average density for each mandible ($R = -0.38$) requires a sample size greater than 25 to be significant at $P = 0.05$. No studies are available using larger samples of dentate mandibles.

Radiographic studies have variable findings regarding site differences in mandibular cortical densities. Hobson and Beynon (1997) use quantitative computed tomography to determine mean mineralization values for 6 edentulous human mandibles at 4 facial and lingual sites. They find no differences among sites, sides, or genders, but their sample size (3 males and 3 females) is small. Maki et al. (2000) also use quantitative computed tomography to assess a larger sample of 16 females and 18 males, ranging from 9 to 33 years old. They conclude that the symphyseal cortex is denser lingually, while the alveolar process and mid- to inferior-ramus is denser facially. Our results support these conclusions.

Reliability of mean material property values in modeling mandibular function or interpreting measured bone strain

Material properties are important in studies of mandibular loading and deformation because cortical bone is anisotropic (Dechow and Hylander, 2000). Variations in material anisotropy and direction of maximum stiffness contribute to error in stress magnitudes and orientations calculated from experimentally measured or modeled bone strains (Carter, 1978; Cowin and Hart, 1990; Cowin et al., 1991; Dechow et al., 1993; Dechow and Hylander, 2000; Ricos et al., 1996; Turner and Cowin, 1988). We examine the reliability of using mean cortical material properties to interpret loading patterns in individual mandibles by looking at the effects of material property variation on 1) the direction of maximum principal stress compared to maximum principal strain, and 2) σ_q/σ_p compared to ϵ_q/ϵ_p .

Reliability varies, depending on region. Some mandibular regions exhibit little variation in mate-

rial properties so that calculations, including mean material property data, yield reasonable estimates of stress. In other regions, these estimates are less reliable because of larger variation in material properties.

Estimates of orientations of principal stresses are only mildly affected by variations in the direction of maximum material stiffness. The largest deviation in orientation between the maximum principal strain and stress ($\Delta\Phi$) is relatively small at $\pm 12.9^\circ$ when $\epsilon_q/\epsilon_p = 1.0$ (Fig. 10A), and increases only marginally to a plateau near 13.2° for $\epsilon_q/\epsilon_p = 3.0$ (Fig. 11A). There is a theoretical maximum error of 45° in principal stress axis orientation, if anisotropic bone is modeled as isotropic (Cowin and Hart, 1990). The error is less in empirical studies of macaque mandibles (Dechow and Hylander, 2000), in which some examples have errors up to 11.6° . In mandibular regions with consistent directions of maximum cortical stiffness (lower border of the mandible, for example), estimates of stress orientations are improved by including mean material property information in the calculations. In regions where anisotropy is large and there is little consistency in the direction of maximum stiffness among individuals (coronoid process), errors in estimating principal stress orientations do not exceed 13.2° .

Errors in calculated σ_q/σ_p are greater depending on both $\Delta\mu$ and E_2/E_3 anisotropy. The magnitude of σ_q/σ_p decreases up to 75% when $E_2/E_3 = 0.5$ (Fig. 10B). Absolute errors in σ_q/σ_p are larger if $\epsilon_q/\epsilon_p > 1.0$ (Fig. 11B). The magnitude of range of anisotropy values is as important as the range of variance itself in determining error for mandibular sites. Sites with larger mean anisotropies have larger errors than those with smaller anisotropies, even if the amount of individual variation at each site was comparable.

Material properties and mandibular function

A central element of our understanding of bone adaptation is that bone loading and deformation influence modeling and remodeling and the resulting microstructural organization (Ascenzi, 1988; Lanyon, 1991; Lanyon and Rubin, 1985; Martin et al., 1998; Skedros et al., 1996; Smit and Burger, 2000). Few studies directly address the question of how directional variations in material properties relate to bone microstructure at a tissue level, although some evidence indicates that directional differences correlate with anisotropies in the mineral component, but not in the organic component (Hasegawa et al., 1994; Turner et al., 1995; Takano et al., 1999). Theoretical studies speculate about ways in which patterns of bone loading may direct osteon orientation during remodeling (Martin et al., 1998; Smit and Burger, 2000) and presumably influence bone anisotropy.

If osteon orientation and other microarchitectural features of bone result at least in part from the effects of functional loading on bone remodeling, and if the direction of maximum stiffness in bone is

dependent on the orientation of the microstructure, then there should be a relationship between the direction of maximum stiffness and the average direction of loading. The problem is that in regions of the skeleton with numerous, complex loading patterns, such as in parts of the mandible, there is no reliable methodology for estimating cumulative patterns of loading. It is not possible to answer questions such as: 1) does low anisotropy indicate that cumulative loading patterns have no dominant direction of stress, or does low anisotropy indicate that a region is simply a low stress region, or are both true in different portions of the skeleton; or 2) does variation in the direction of maximum stiffness reflect functional differences among individuals, or does such variation reflect regions with low stresses.

Here we review some of the regional cortical bone characteristics of the mandible and attempt to relate these to mandibular function. Such an analysis is limited by the lack of information on in vivo mandibular strains during masticatory function in humans, although loading patterns can be inferred from ex vivo strain and finite element studies of human mandibles, and in vivo experiments using nonhuman primate models (van Eijden, 2000).

Symphysis. Within the symphysis, at least three distinct loading patterns produce stress (Daegling, 1993; Hylander, 1984; van Eijden, 2000; Wolff, 1984): 1) lateral transverse bending places compression on the facial cortex and tension on the lingual cortex, 2) frontal or vertical bending places tension on the inferior border and compression on the alveolar process, and 3) torsion between working and balancing sides contributes to dorsoventral and anteroposterior shear. Mandibular features, which resist deformation at the symphysis, include a broad symphyseal height and width, and a relatively short mandibular length.

Material properties suggest possible correlations with symphyseal stress patterns. For example, the thick cortex of the inferior border occurs where the greatest tensile stresses are likely to be found during vertical bending. Cortical density is also greater on the human symphyseal lingual cortex, where presumed lateral transverse bending places the largest tensile loads. Bone on the compressed facial cortex is less dense and also has more nonoriented sites. This finding is contrary to studies on the calcaneus of sheep and deer (Skedros et al., 1994), in which greater cortical porosity (less density) is associated with regions of greater tension.

It is difficult to make definitive statements about relationships between cortical microstructure and function in the human mandible, as our understanding of loading patterns associated with individual functions as well as of the cumulative effects of multiple loading patterns over time is limited. More is known about variations in functional loading in the mandibles of nonhuman primate models (Hylander, 1984). However, these studies are not neces-

sarily a good analog for understanding loading patterns in humans, because of shape differences between species. But it is reasonable to suggest similar ranges of variation.

It is interesting that the direction of maximum stiffness is highly variable at the symphysis. The lower border and some midbody sites have significant orientations and anisotropies, while alveolar sites and some midbody sites have no significant orientation among individuals and little anisotropy. If principal material orientation and loading are related, these data suggest that symphyseal loading 1) is complex and lacks a predominate pattern, particularly in the alveolar region; and/or 2) is markedly variable among individuals, reflecting variations in individual functional habits and morphologies.

Corpus. Strain gage studies in macaques and baboons, as well as finite element models in humans, suggest that the mandibular corpus experiences complex loads during function (Hylander, 1984; Kabel et al., 1999; Koriath et al., 1992). Patterns of midcorpus bone geometry (Daegling and Hylander, 1998), as well as variations in the direction of maximum stiffness and material properties (Dechow and Hylander, 2000), may contribute to these complex patterns of corpus loading and deformation.

In a study of elastic properties and in vitro strain in macaque mandibles, Dechow and Hylander (2000) found stress patterns that suggest parasagittal bending on the balancing side, with the lower border in compression and some secondary torsion. On the working side, patterns suggest torsion coupled with superimposed patterns of parasagittal and lateral transverse bending or direct shear (Daegling and Hylander, 1998, 2000; Hylander, 1979a-c). It is interesting that the average facial working side ϵ_q angle of 35.3° in macaques is similar to the average direction of maximum stiffness (34.8°) in similar regions of the human corpus. The correspondence of ϵ_q angle and material property orientation indicates that at the lower border of the facial cortex, the bone is well-adapted to resist superimposed bending and torsional stresses. However, the average lingual working side ϵ_q angle of 22.9° is steeper than the direction of maximum stiffness throughout the lingual corpus, where the average direction of maximum stiffness is 8.3°. Whether this reflects functional differences between the macaque and human masticatory systems, or whether macaques also have this difference in facial and lingual material properties, requires further study.

There is an interesting controversy regarding the relative strain magnitudes experienced between the alveolar process and inferior border of the mandibular corpus. Photoelastic and finite element studies suggest that occlusal loads lead to concentrations of strain in the alveolar process (Andersen et al., 1991a,b; Hood et al., 1975; Koriath et al., 1992; Koriath and Versluis, 1997). However, in vitro strain gage studies of human mandibles refute this, since

strain concentrations distribute evenly when bite and muscle forces occur in unison (Daegling and Hylander, 2000), which supports the closed beam model of response to torsional loads (Chen and Chen, 1998; Daegling and Grine, 1991). In this study, the uniformity of material properties, including density, may imply that cortical bone is adapted to loads that are well-distributed between the alveolar process and inferior border. Both elastic and shear moduli are similar between the alveolar process and inferior border. However, the facial cortex often has significantly larger values of elastic and shear moduli compared to the lingual cortex (Table 6). These material property differences and cortical thickness, especially within the submandibular fossa, may suggest differences in the functional environment of the lingual cortex.

Ramus. Complex direct muscle forces, bony deformation, and reactive joint forces influence the strain environment of the ramus, condylar process, and coronoid process. Facial ramus sites are thicker and often have greater elastic and shear moduli than lingual sites, suggesting a possible correlation with greater loads.

Few *in vivo* strain gage data are available for the ramus, since the placement of gauges significantly disrupts the functional environment (Hylander, 1979c; Liu and Herring, 2000; Teng and Herring, 1998). Hylander (1979b), using strain gauges *in vivo* on the macaque lateral condylar region, demonstrates widely varying magnitudes and orientations of compressive and tensile strain, depending on the bite point position. The average macaque condylar neck ϵ_q angles of 65° and 78° are similar to the average human direction of maximum stiffness (63°), but as in the corpus, they are dissimilar lingually. Large variation in strain on the lateral condylar neck is also found in miniature pigs (Liu and Herring, 2000). An *in vitro* strain gage study on the condylar neck of unembalmed human mandibles (Throckmorton and Dechow, 1994) also shows ϵ_q angles that are similar to the direction of maximum stiffness facially, but less similar lingually.

CONCLUSIONS

1. The direction of maximum stiffness, cortical thickness, cortical density, and elastic properties for the dentate human mandible demonstrate unique regional variation (Table 6).
2. The orientation of elastic properties might be explained by the orientation of cortical bone microstructure. A major component of this microstructure which qualitatively corresponds to material orientation is the direction of osteons, as suggested by split-line studies. However, data in this area are sparse. Actual measurements of osteon orientations and their variations, compared with information about tissue-level three-dimensional cortical material properties, do not exist.
3. Specific relationships between material proper-

ties and mandibular function remain elusive. How this variation in material properties is modeled during growth or maintained throughout life awaits further study.

4. The accuracy of stresses calculated from strains and elastic properties varies regionally and depends on variation among individuals in the direction of maximum stiffness and anisotropy. Stresses in some parts of the mandible can be more accurately calculated than in other regions.

ACKNOWLEDGMENTS

We thank Drs. Peter Buschang, Richard Harper, Gaylord Throckmorton, and three anonymous reviewers for their comments regarding this study.

LITERATURE CITED

- Andersen KL, Mortensen HT, Pedersen EH, Melsen B. 1991a. Determination of stress levels and profiles in the periodontal ligament by means of an improved three-dimensional finite element model for various types of orthodontic and natural force systems. *J Biomed Eng* 13:293–303.
- Andersen KL, Pedersen EH, Melsen B. 1991b. Material parameters and stress profiles within the periodontal ligament. *Am J Orthod Dentofacial Orthop* 99:427–440.
- Arendts FJ, Sigolotto C. 1990. Mechanical characteristics of the human mandible, and investigation of the “*in-vivo*” reaction of the compact bone: a contribution to the description of the biomechanics of the mandible—part II. *Biomed Tech* 35:123–130.
- Ascenzi A. 1988. The micromechanics versus the macromechanics of cortical bone—a comprehensive presentation. *J Biomech Eng* 110:357–363.
- Ashman RB, van Buskirk WC. 1987. The elastic properties of a human mandible. *Adv Dent Res* 1:64–67.
- Ashman RB, Cowan SC, van Buskirk WC, Rice JC. 1984. A continuous wave technique for measurement of the elastic properties of cortical bone. *J Biomech* 17:349–361.
- Ashman RB, Rosinia G, Cowin SC, Fontentot MG, Rice JC. 1985. The bone tissue of the canine mandible is elastically isotropic. *J Biomech* 18:717–721.
- Asundi A, Kishen A. 2000. A strain gauge and photoelastic analysis of *in vivo* strain and *in vitro* stress distribution in human dental supporting structures. *Arch Oral Biol* 45:543–550.
- Benninghoff A. 1925. Spaltlinien am Knochen, eine Methode zur Ermittlung der Architektur platter Knochen. *Verh Anat Ges* 34:189–206.
- Bouvier M, Hylander WL. 1981. The relationship between split-line orientation and *in vivo* bone strain in galago (*G. crassicaudatus*) and macaque (*Macaca mulatta* and *M. fascicularis*) mandibles. *Am J Phys Anthropol* 56:147–156.
- Bouvier M, Hylander WL. 1996. The mechanical or metabolic function of secondary osteonal bone in the monkey *Macaca fascicularis*. *Arch Oral Biol* 41:941–950.
- Buckland-Wright JC. 1977. Microradiographic and histological examination of the split-line formation in bone. *J Anat* 124:193–203.
- Carter DR. 1978. Anisotropic analysis of strain rosette information from cortical bone. *J Biomech* 11:199–202.
- Carter C. 1989. The elastic properties of the human mandible. Ph.D. thesis, Tulane University, New Orleans, LA.
- Chen X, Chen H. 1998. The influence of alveolar structures on the torsional strain field in a gorilla corporeal cross-section. *J Hum Evol* 35:611–633.
- Cowin SC. 1989. The mechanical properties of cortical bone tissue. In: Cowin SC, editor. *Bone mechanics*. Boca Raton, FL: CRC Press. p 98–124.
- Cowin SC, Hart RT. 1990. Errors in the orientation of the principal stress axes if bone tissue is modeled as isotropic. *J Biomech* 23:349–352.

- Cowin SC, Sadegh AM, Luo GM. 1991. Correction formulae for the misalignment of axes in the measurement of the orthotropic elastic constants. *J Biomech* 24:637–641.
- Daegling DJ. 1993. Functional morphology of the human chin. *Evol Anthropol* 1:170–177.
- Daegling DJ, Grine FE. 1991. Compact bone distribution and biomechanics of early hominid mandibles. *Am J Phys Anthropol* 86:321–339.
- Daegling DJ, Hylander WL. 1998. Biomechanics of torsion in the human mandible. *Am J Phys Anthropol* 105:73–87.
- Daegling DJ, Hylander WL. 2000. Experimental observation, theoretical models, and biomechanical inference in the study of mandibular form. *Am J Phys Anthropol* 112:541–551.
- Dechow PC, Hylander WL. 2000. Elastic properties and masticatory bone stress in the macaque mandible. *Am J Phys Anthropol* 112:553–574.
- Dechow PC, Schwartz-Dabney CL, Ashman RB. 1992. Elastic properties of the human mandibular corpus. In: Carlson DS, Goldstein SA, editors. *Bone biodynamics in orthodontic and orthopedic treatment*. Ann Arbor, MI: Center for Human Growth and Development. p 299–314.
- Dechow PC, Nail GA, Schwartz-Dabney CL, Ashman RB. 1993. Elastic properties of human supraorbital and mandibular bone. *Am J Phys Anthropol* 90:291–306.
- Demes B, Qin Y-X, Stern JT Jr, Larson SG, Rubin CT. 2001. Patterns of strain in the macaque tibia during functional activity. *Am J Phys Anthropol* 116:257–265.
- Duterloo HS, Atkinson PJ, Woodhead C, Strong M. 1974. Bone density changes in the mandibular cortex of the rhesus monkey *Macaca mulatta*. *Arch Oral Biol* 19:241–248.
- Endo B. 1973. Stress analysis on the facial skeleton of gorilla by means of the wire strain gauge method. *Primates* 14:37–45.
- Evans FG. 1973. Preservation effects. In: Evans FG, editor. *Mechanical properties of bone*. Springfield, IL: Charles C. Thomas. p 56–60.
- Fratzl P, Groschner M, Vogl G, Plenk H Jr, Eschberger J, Fratzl-Zelman N, Koller K, Klaushofer K. 1992. Mineral crystals in calcified tissues: a comparative study by SAXS. *J Bone Miner Res* 7:329–334.
- Giesen EBW, van Eijden TMGJ. 2000. The three-dimensional cancellous bone architecture of the human mandibular condyle. *J Dent Res* 79:957–963.
- Giesen EBW, Ding M, Dalstra M, van Eijden TMGJ. 2001. Mechanical properties of cancellous bone in the human mandibular condyle are anisotropic. *J Biomech* 34:799–803.
- Hara T, Takizawa M, Sato T, Ide Y. 1998. Mechanical properties of buccal compact bone of the mandibular ramus in human adults and children: relationship of the elastic modulus to the direction of the osteon and the porosity ratio. *Bull Tokyo Dent Coll* 39:47–55.
- Hart RT, Hennebel VV, Thongpreda N, van Buskirk WC, Anderson RC. 1992. Modeling the biomechanics of the mandible: a three-dimensional finite element study. *J Biomech* 25:261–286.
- Hasegawa K, Turner CH, Burr DB. 1994. Contribution of collagen and mineral to the elastic anisotropy of bone. *Calcif Tissue Int* 55:381–386.
- Henrikson PA, Wallenius K. 1974. The mandible and osteoporosis (1). *J Oral Rehabil* 1:67–74.
- Herzberg F, Dovitch V. 1968. Bony trabecular changes in the human mandibular ramus from prenatal period to adulthood. *Anat Rec* 161:517–522.
- Hobson RS, Beynon AD. 1997. Preliminary quantitative microradiography study into the distribution of bone mineralization within the basal bone of the human edentulous mandible. *Arch Oral Biol* 42:497–503.
- Hood JAA, Farah JW, Craig RG. 1975. Modification of stresses in alveolar bone induced by a tilted molar. *J Prosthet Dent* 34:415–421.
- Hylander WL. 1979a. An experimental analysis of the temporomandibular joint reaction force in macaques. *Am J Phys Anthropol* 51:433–456.
- Hylander WL. 1979b. Mandibular function in *Galago crassicaudatus* and *Macaca fascicularis*: an in vivo approach to stress analysis of the mandible. *J Morphol* 159:253–296.
- Hylander WL. 1979c. The functional significance of primate mandibular form. *J Morphol* 160:223–240.
- Hylander WL. 1984. Stress and strain in the mandibular symphysis of primates: a test of competing hypotheses. *Am J Phys Anthropol* 64:1–46.
- Hylander WL, Johnson KR, Crompton AW. 1987. Loading patterns and jaw movements during mastication in *Macaca fascicularis*: a bone-strain, electromyographic, and cineradiographic analysis. *Am J Phys Anthropol* 72:287–314.
- Kabel J, Van Rietbergen B, Dalstra M, Odgaard A, Huiskes R. 1999. The role of an effective isotropic tissue modulus in the elastic properties of cancellous bone. *J Biomech* 32:673–680.
- Kaewsuriyathumrong C, Soma K. 1993. Stress of tooth and PDL structure created by bite force. *Bull Tokyo Med Dent Univ* 40:217–232.
- Katz JL, Meunier A. 1987. The elastic anisotropy of bone. *J Biomech* 20:1063–1070.
- Katz JL, Yoon HS, Lipson S, Maharidge R, Meunier A, Christel P. 1984. The effects of remodeling on the elastic properties of bone. *Calcif Tissue Int* 36:31–36.
- Kohles SS, Bowers JR, Vailas AC, Vanderby R Jr. 1997. Ultrasonic wave velocity measurement in small polymeric and cortical bone specimens. *J Biomech Eng* 119:232–236.
- Korioth TWP, Versluis A. 1997. Modeling the mechanical behavior of the jaws and their related structures by finite element (FE) analysis. *Crit Rev Oral Biol Med* 8:90–104.
- Korioth TWP, Romilly DP, Hannam AG. 1992. Three-dimensional finite element stress analysis of the dentate human mandible. *Am J Phys Anthropol* 88:69–96.
- Lanyon LE. 1991. Biomechanical properties of bone and response of bone to mechanical stimuli: functional strain as a controlling influence on bone modeling and remodeling behavior. In: Hall BK, editor. *Bone matrix and bone specific products*. London: CRC Press, Inc. p 79–108.
- Lanyon LE, CT Rubin. 1985. Functional adaptation in skeletal structures. In: Hildebrand M, Bramble DM, Liem KF, Wake DB, editors. *Functional vertebrate morphology*. Cambridge, MA: Belknap Harvard Press. p 1–25.
- Lipson SF, Katz JL. 1984. The relationship between elastic properties and microstructure of bovine cortical bone. *J Biomech* 17:231–240.
- Liu ZJ, Herring SW. 2000. Bone surface strains and internal bony pressures at the jaw joint of the miniature pig during masticatory muscle contraction. *Arch Oral Biol* 45:95–112.
- Maki K, Miller A, Okano T, Shibasaki Y. 2000. Changes in cortical bone mineralization in the developing mandible: a three-dimensional quantitative computed tomography study. *J Bone Miner Res* 15:700–709.
- Marks L, Teng S, Artun J, Herring S. 1997. Reaction strains on the condylar neck during mastication and maximum muscle stimulation in different condylar positions: an experimental study in the miniature pig. *J Dent Res* 76:1412–1420.
- Martin RB, Burr DB, Sharkey NA. 1998. *Skeletal tissue mechanics*. New York: Springer.
- Meijer HJA, Starmans FJM, Steen WHA, Bosman F. 1993. A three-dimensional, finite-element analysis of bone around dental implants in an edentulous human mandible. *Arch Oral Biol* 38:491–496.
- Petrtyl M, Hert J, Fiala P. 1996. Spatial organization of the Haversian bone in man. *J Biomech* 29:161–169.
- Reilly DT, Burstein AH. 1974. The mechanical properties of cortical bone—review article. *J Bone Joint Surg [Am]* 56:1001–1021.
- Rho J-Y. 1996. An ultrasonic method for measuring the elastic properties of human tibial cortical and cancellous bone. *Ultrasonics* 34:777–783.
- Ricos V, Pedersen DR, Brown TD, Ashman RB, Rubin CT, Brand RA. 1996. Effects of anisotropy and material axis registration on computed stress and strain distributions in the turkey ulna. *J Biomech* 29:261–267.
- Schwartz-Dabney CL. 2001. Cortical material properties of the human dentate and edentulous mandible. Ph.D. thesis, Baylor College of Dentistry, Texas A&M University System Health Science Center, Dallas, TX.

- Seipel CM. 1948. Trajectories of the jaws. *Acta Odontol Scand* 8:81–191.
- Shinedling EA, Dechow PC. 1996. Elastic properties of mandibular cortical bone in neonatal pigs. *J Dent Res* 75:798 [abstract].
- Skedros JG, Mason MW, Nelson MC, Bloebaum RD. 1996. Evidence of structural and material adaptation to specific strain features in cortical bone. *Anat Rec* 246:47–63.
- Smit TH, Burger EH. 2000. Is BMU-coupling a strain-regulated phenomenon? A finite element analysis. *J Bone Miner Res* 15:301–307.
- Takano Y, Turner CH, Owan I, Martin RB, Lau ST, Forwood MR, Burr DB. 1999. Elastic anisotropy and collagen orientation of osteonal bone are dependent on the mechanical strain distribution. *J Orthop Res* 17:59–66.
- Tamatsu Y, Kaimoto K, Arai M, Ide Y. 1996. Properties of the elastic modulus form buccal compact bone of the human mandible. *Bull Tokyo Dent Coll* 37:93–101.
- Tappen NC. 1954. A comparative functional analysis of primate skulls by the split-line technique. *Hum Biol* 26:220–238.
- Tappen NC. 1967. Some relationships between split-line patterns and underlying structure in primate skeletons. In: Starck DR, Schneider R, Kuhn H-J, editors. *Neue Ergebnisse der Primatologie* [Progress in primatology]. Stuttgart: Gustav Fischer Verlag. p 80–89.
- Tappen NC. 1970. Main patterns and individual differences in baboon skull split-lines and theories of causes of split-line orientation in bone. *Am J Phys Anthropol* 33:61–72.
- Teng S, Herring SW. 1995. A stereological study of trabecular architecture in the mandibular condyle of the pig. *Arch Oral Biol* 40:299–310.
- Teng S, Herring SW. 1996. Anatomic and directional variation in the mechanical properties of the mandibular condyle in pigs. *J Dent Res* 75:1842–1850.
- Teng S, Herring SW. 1998. Compressive loading on bone surfaces from muscular contraction: an in vivo study in the miniature pig, *Sus scrofa*. *J Morphol* 238:71–80.
- Thomason JJ, Grovum LE, Deswysen AG, Bignell WW. 2001. *In vivo* surface strain and stereology of the frontal and maxillary bones of sheep: implications for the structural design of the mammalian skull. *Anat Rec* 264:325–338.
- Throckmorton GS, Dechow PC. 1994. In vitro strain measurements in the condylar process of the human mandible. *Arch Oral Biol* 39:853–867.
- Throckmorton GS, Ellis E III, Winkler AJ, Dechow PC. 1992. Bone strain following application of a rigid bone plate: an in vitro study in human mandibles. *J Oral Maxillofac Surg* 50:1066–1073.
- Turner CH, Cowin SC. 1988. Errors induced by off-axis measurement of the elastic properties of bone. *J Biomech Eng* 110:213–215.
- Turner CH, Chandran A, Pidaparti RMV. 1995. The anisotropy of osteonal bone and its ultrastructural implications. *Bone* 17:85–89.
- van Buskirk WC, Cowin SC, Ward RN. 1981. Ultrasonic measurement of orthotropic elastic constants of bovine femoral bone. *J Biomech Eng* 103:67–72.
- van Eijden TMGJ. 2000. Biomechanics of the mandible. *Crit Rev Oral Biol Med* 11:123–136.
- Weiner S, Traub W, Wagner HD. 1999. Lamellar bone: structure-function relations. *J Struct Biol* 126:241–255.
- Wirtz DC, Schiffers N, Pandorf T, Radermacher K, Weichert D, Forst R. 2000. Critical evaluation of known bone material properties to realize anisotropic FE-simulation of the proximal femur. *J Biomech* 33:1325–1330.
- Wolff JEA. 1984. A theoretical approach to solve the chin problem. In: Chivers DJ, Wood BA, Bilsborough A, editors. *Food acquisition and processing in primates*. New York: Plenum Press. p 391–405.
- Zar JH. 1996. Circular distributions: descriptive statistics. In: Zar JH, editor. *Biostatistical analysis*. Upper Saddle River, New Jersey: Prentice-Hall, Inc. p 519–611.
- Ziopoulos P, Currey JD. 1998. Changes in the stiffness, strength and toughness of human cortical bone with age. *Bone* 22:57–66.
- Ziopoulos P, Smith CW, An YH. 2000. Factors affecting mechanical properties of bone. In: An RA, Draughn RA, editors. *Mechanical testing of bone and the bone-implant interface*. New York: CRC Press. p 65–85.